Paleoenvironmental study of modern charcoal making activity on forest soils in the Northern Vosges Mountains (Bitche, France): A multidisciplinary study of two remaining charcoal platforms and associated soils sequences

Anne Gebhardt, Anne Poszwa, Laurence Mansuy-Huault, Vincent Robin, Luc Vrydaghs, Catherine Lorgeoux

Received: 7 March 2023 | Revised: 3 November 2023 | Accepted: 6 November 2023

DOI: 10.1002/gea.21986

RESEARCH ARTICLE

Geoarchaeology An International Journal WILEY

'Paleoenvironmental study of modern charcoal making activity on forest soils in the Northern Vosges Mountains (Bitche, France): A multidisciplinary study of two remaining charcoal platforms and associated soils sequences'

Anne Gebhardt[1,2,3] | Anne Poszwa[1] | Laurence Mansuy-Huault[1] | Vincent Robin[1] | Luc Vrydaghs[4] | Catherine Lorgeoux[5]

[1]Laboratoire Interdisciplinaire des Environnements Continentaux (LIEC), UMR CNRS 7360, Vandoeuvre-lès-Nancy, France

[2]Laboratoire Image Ville Environnement (LIVE), Université de Strasbourg, Strasbourg, France

[3]Institut National de Recherche en Archéologie Préventive (INRAP), France

[4]Multidisciplinary Archaeological Research Institute (MARI), Vreije Universiteit Brussel (VUB), Brussel, Belgium

[5]Georessources, Vandoeuvre-lès-Nancy, France

Correspondence
Anne Gebhardt, Laboratoire Interdisciplinaire des Environnements Continentaux (LIEC), UMR CNRS 7360, Site Aiguillette, Université de Lorraine, Faculté des Sciences et Technologies, BP 70239, FR-54506 Vandoeuvre-lès-Nancy, France.
Email: anne.gebhardt-even@inrap.fr

Scientific editing by Kevin Walsh

Abstract

This multidisciplinary study aims to decipher the impact of ancient charcoal production on past and present-day soils in the northern Vosges Mountains. Soil observations in the field and laboratory were complemented by charcoal and phytolith studies on large thin sections, molecular analyses of organic pollutants, and phytolith analysis on bulk samples. The complex *technosol* platform records an ancient natural soil sequence buried by a human-made platform on which charcoal accumulated. The current upslope soil is an *entic Podzol*. Palaeoecological data collected in the buried soil are reliable owing to low bioactivity due to soil acidity. Podzolisation predated the platform construction. The presence of ashes induced low soil alkalisation developed in the charcoal hearth remains and appears to have generated the migration of subsequent iron/clay/organic bands throughout the platform sediment and the buried soil. Charcoal studied in thin sections revealed mainly *Quercus* and *Fagus* taxa. Phytolith studies suggest that a less dense or degraded forest preceded platform construction, probably due to former woodland coppicing or earlier disorganised wood gathering. The specific distribution of polycyclic aromatic hydrocarbons sorbed on charcoal has persisted in soils throughout centuries, but we have no evidence that charcoal-making activities contributed to diffuse global pollution.

KEYWORDS

charcoal platforms, forest soils, historical ecology, north-eastern France, phytoliths, polycyclic aromatic hydrocarbons

1 | INTRODUCTION

This paper presents the analysis of soil profiles associated with two relict charcoal hearths located in the northern part of the Vosges Mountains (Bitche, France; Figure 1), an area known for its important charcoal production since the 17th century. In this paper, to avoid confusing terminology, the terms charcoal hearth or charcoal mound will be used to refer to the residues of charcoal production from nonpermanent installations (Gebhardt, 2007; Hirsch et al., 2017), rather than charcoal kilns, which designate specific brick/stone/metal permanent constructions (Food and Agriculture Organization of the United Nations, 1987; Padiam & McDonald, 1987; Pitts Jarvis, 1960; Schlosser, 2021), or mobile metallic pans (Calvet, 2012) used for charcoal production. Here, the term platform refers to the flat surface levelled on a slope to support the charcoal mound.

Most previous charcoal hearth investigations have focused on charcoal identification and dating to assess the human impact on changes in vegetation and coppice wood exploitation cycles (Deforce et al., 2018; Dupin et al., 2017; Fouédjeu et al., 2021; Gocel-Chalté et al., 2020; Ludemann et al., 2017; Oliveira et al., 2022). Some projects have addressed the role of black carbon and charcoal as carbon sinks in soils (Bell & Worrall, 2011; Borchard et al., 2014; Bourne et al., 2014; Hardy et al., 2017). However, only a few references discuss the long-term effects of charcoal production sites on soil fertility (Rodrigues et al., 2019), with mentions of reacidification and the depletion of exchangeable K^+ and available P in the topsoil (Bonhage et al., 2020; Hardy et al., 2017; Hirsch et al., 2017).

Papers focusing on the fertilising impact of charcoal are more frequent (Barbosa et al., 2006; Kerré et al., 2017; Mastrolonardo et al., 2018; De Resende et al., 2018; Rodrigues et al., 2019). Charcoal production activity generates by-products, including significant amounts of tar (10% of the produced charcoal in the experiment of Fagernas et al. [2012]). These tars are enriched in polycyclic aromatic compounds (PACs), 16 of which are identified as priority pollutants (regulatory polycyclic aromatic hydrocarbons [PAHs]) (Fagernas et al., 2012; Wang et al., 2017). Due to their hydrophobic and refractory properties, they are persistent in soils and can be used as organic tracers of charcoal activity and other biomass thermal conversion processes (Conedera et al., 2009).

Research into charcoal platform (CP) construction and traditional charcoal production's impact on the underlying sequence's pedogenetic evolution is rarer (Gebhardt, 2007; Hirsch et al., 2017; Raab et al., 2019). For practical (access) and safety reasons (fire), demonstration recreational charcoal mounds are constructed in nonforested meadows or already strongly transformed soils (artificial dumps, car park areas, etc.). Therefore, they cannot be used as real references to address the impact of charcoal burners on associated forest soils. Their potential to provide comparative environmental and ecological data is limited.

The need for charcoal has strongly influenced the evolution of the Bitscherland forest since early medieval times (Gocel-Chalté et al., 2020). After attracting the first monastic settlements to the area during the 12th century, water availability and forest resources favoured glassworking from the 15th century onwards, while iron-working forges developed during the 17th/18th centuries (Jehin, 2005; Rochel, 2017). The steel industry used wood charcoal until the arrival of coal. According to Jehin (2005), producing one ton of cast iron required around 15,000 m^3 of charcoal, representing between 30,000 and 45,000 steres of wood (one stere is around 1 m^3 of 1-m-long piled wooden logs). This huge quantity of wood

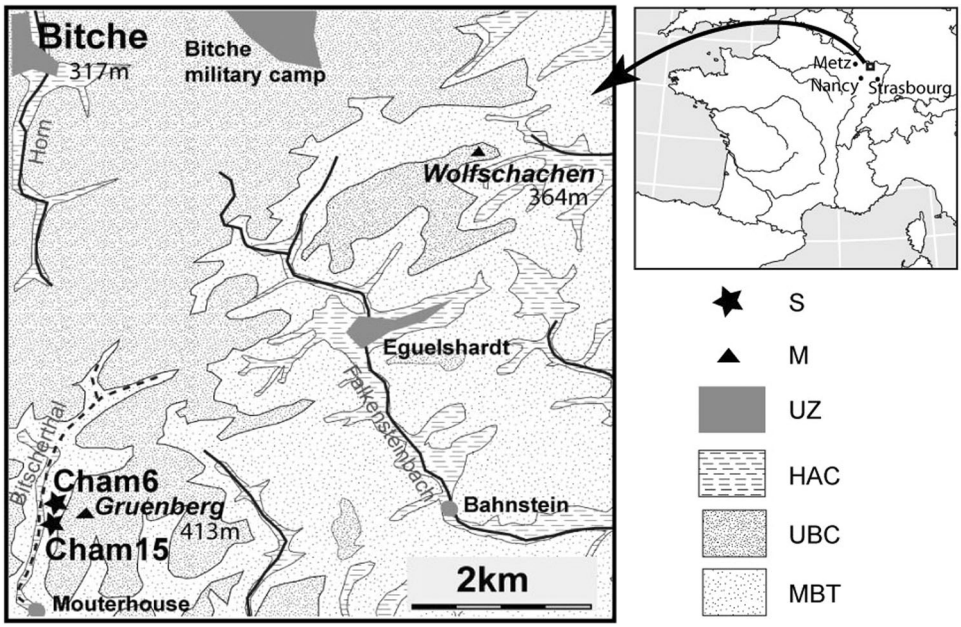

FIGURE 1 Location of the sites on the geological map (after Menillet et al., 1989). HAC, Holocene Alluvial and Colluvial valley deposits; M, mountain; MBT, Middle Buntsandstein Triffels layers; S, sites; UBC, Upper Buntsandstein Conglomerate; UZ, urban zones.

extraction was based on long-term sustainable forest management and the organisation of charcoal production. According to the general literature, coppicing rotation averages from 20 (Hardy & Dufey, 2012) to 30 years (Garnier, 2004; Nolken, 2005). For Bitscherland, forestry archives from the 18th century recount a long but complex coppicing rotation rate of about 50 years, in coppice with standards, with local variations (Rochel, 2017).

Furthermore, a topographical atlas of the county of Bitche, dating from 1758, illustrates a precise map of forest cover in the mid-18th century (original archive: Anonymous, 1758; transcriptions: Robin, 2006; Rochel, 2017). The Cham6/Cham15 areas on the Gruenberg slopes reveal an acid, heather-covered and generally treeless environment, with locally sparse, mostly dry dead-capped oaks, poor-quality coppice and birch. In this atlas, there is no mention of wood for charcoal production, although, in the whole of the Bitche region, the density of CPs in the study area varies from 0.35 to 0.52 per hectare (Gocel-Chalté et al., 2020). We may assume that, on the Gruenberg, the charcoal-making activities began after 1758.

In his 'charcoal making art', Duhamel du Monceau (1761) suggests finding a flat round place with no organic elements (roots, twigs, leaves, ancient charcoal pieces, etc.) to sustain the slow reduced combustion process perfectly. The use of digging tools to clean and prepare the site (Burri, 2008) deeply impacts not only the natural soil structure under the charcoal hearth (Gebhardt, 2007, 2008) but also around it if platform construction is necessary (Gebhardt, 2021). To avoid digging, minerogenic sediments can be accumulated to seal the natural soil on a flat area, level a slope or raise the ground of an eroded platform. Moreover, previous locations were often reused, which is logical when considering the heavy work required to construct platforms. Between each combustion episode, the platform surface needed to be scraped and cleaned to remove residual charcoal or organic debris. After combustion, the fine mix of sediment, ash and charcoal residues, called *frasil* in old French (Duhamel du Monceau, 1761), was scraped and reused from one charcoal mound to another to properly seal the holes between the wooden logs and maintain the combustion in a reduced atmosphere. This potential charcoal movement between CPs needs to be taken into account during charcoal hearth studies and dating. On slopes, CPs are constructed in a typical 'step-like' shape (Figure 2), and terracing also strongly impacts local morphology and soils.

The work presented here is part of several projects that ran from 2018 to 2020, aiming to enhance our understanding of the impact of ancient charcoal production on soils. This paper focuses on comparing the pedogenetic evolution of two well-preserved

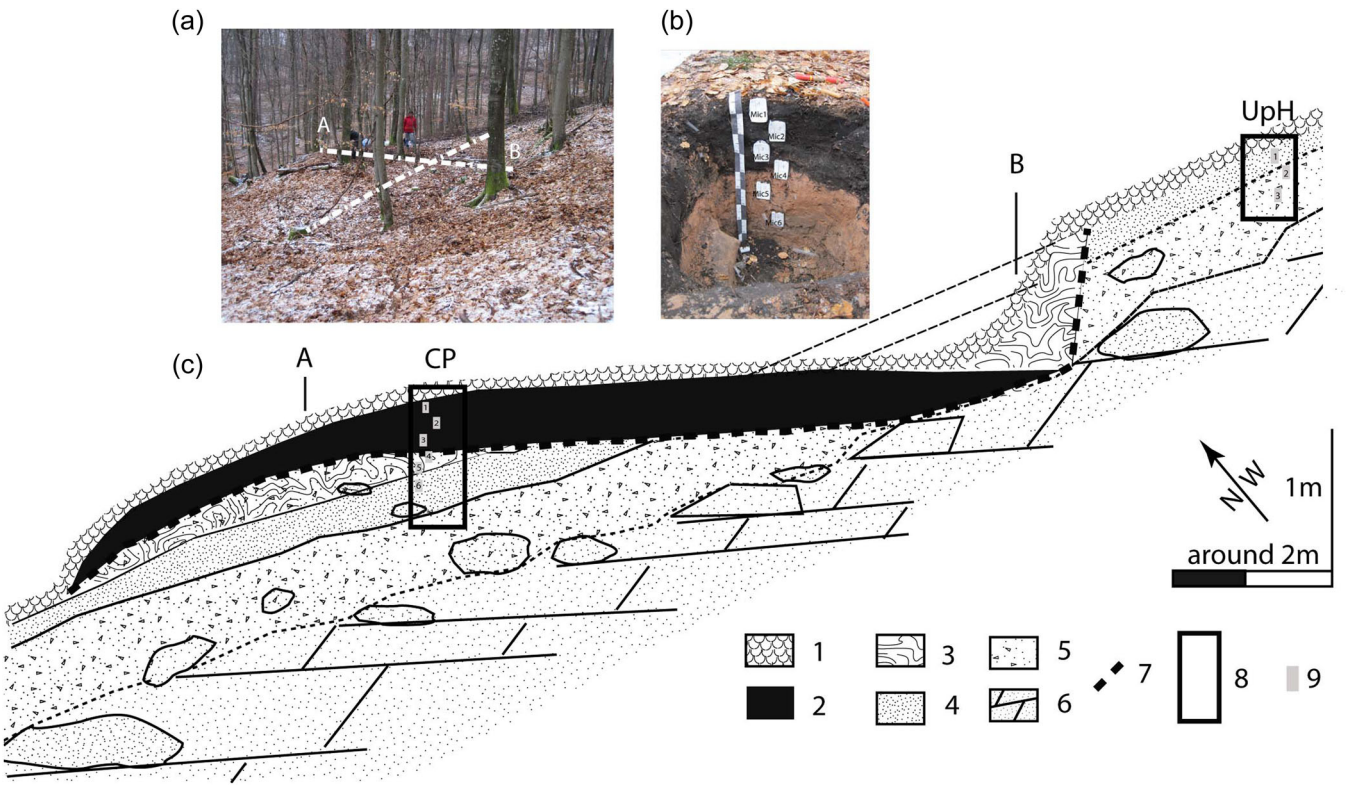

FIGURE 2 General organisation of the site with location of the charcoal platform (CP) and Uphill reference (UpH) profiles. (a) View of the studied platform (white dotted lines: diameters of the CP), (b) CP sampled profile, (c) sketch of the CP profile A-B: 1. OL/OFZo organic horizons; 2. U1 last combustion residues; 3. U3 reddish dumped sand forming the platform; 4. U4 greyish sand from the buried palaeosol; 5. U5 red colluvial sand from local Triassic sandstone; 6. weathered Triassic sandstone; 7. platform original profile; 8. location of the pedological pits; 9. location of the undisturbed samples.

CP sequences (Cham6 and Cham15) and their associated present-day uphill soils (UpH). The novelty of the present approach resides in (i) a combination of soil chemical and micromorphological analysis, with charcoal identifications and PAC measurements at the charcoal unit surface (which are combustion residues), (ii) the study of phytoliths on both thin sections and bulk samples and (iii) the analysis on thin sections of charcoal evolution throughout one profile. The results illustrate to what extent charcoal-making activities interacted with natural soil properties and pedogenetic evolution.

2 | MATERIALS AND METHODS

2.1 | Site presentation

The Bitche area (Figure 1, Moselle, France) is a small 350–400-m-high mountain of red ferrous Vosgian Triassic sandstone dating from the middle of Buntsandstein. The horizontally bedded upper part seldom includes quartzite pebbles and manganese nodules, which are absent from the lower-sloping parts. Apart from quartz sand grains, it includes 20% or more of feldspar weathered into kaolinite and muscovite in some fine laminations (Théobald et al., 1967). This hard sandstone's gently west-sloping monoclinal structure gives this hilly landscape its typical tabular shape, surrounded by small wet valleys. A colluviated weathered sandstone deposit covers the steep slopes (20%–25%).

The local climate is oceanic, with continental influences and well-marked seasons (Lexa-Chomard & Pautrot, 2006; Sell et al., 1998). Vegetation cover is a mixed deciduous woodland of beech (*Fagus sylvatica* L.), oak (*Quercus*), ash (*Fraxinus excelsior* L.) and maple (*Acer*), with some conifers (pine [*Pinus sylvestris* L.], spruce [*Picea abies* (L.) H. Karst]) on north-facing slopes and alder (*Alnus*) on low wet ground. The sandy soils, rich in quartz and poor in clay, are acidic and well-drained. Around 40% of soil covers are *podzol*, including 10% of *entic podzols* (Maillant et al., 2016). These morphological and pedological characteristics have curbed the development of agriculture throughout the area (Jamagne, 2011).

The Cham6 CP, dated between 1664 and 1950 cal. A.D. is located at an altitude of 400 m, about 100 m south of the undated Cham15 platform. Both are situated on the slope with a horizontal semicircular surface of 4–6 m diameter and are stratified CPs (Figure 2). The associated comparative present-day UpH soils are 15 m above Cham6.

2.2 | Fieldwork

One pit was opened in the middle of each CP down to the weathered sandstone and, for comparative purposes, in the supposedly undisturbed UpH present-day soil. As our aim was to compare reference profiles (undisturbed soils) with CP profiles, for the profile description, we used the term 'unit', whatever their archaeological or pedological origin. Each profile was described as a succession of units (U). Following pedosedimentary criteria, these units were interpreted and grouped into sequences (S) corresponding to homogeneous sedimentary or pedogenetic phases (Gebhardt et al., 2014). Sequence limits are boundaries resulting from changes in sedimentary (depositional) or pedological processes (Figure 3). The description of soil units (Tables 1 and 2) is based on standard macroscopic criteria (colour, texture, structure, etc.; Baize & Jabiol, 1995; Duchaufour, 1983). For this reason, we treat the soils (UpH) and the remains of the former charcoal-making platform (CP) differently.

For laboratory investigations, undisturbed sediment blocks for soil micromorphological observation and bulk samples for binocular studies, phytolith, physicochemical and organic chemistry analyses were extracted from each unit of the profiles.

2.3 | Laboratory analysis

Colour and binocular observations on bulk air-dried samples supplemented fieldwork observations. Colours were named according to the Munsell transcription of the Revised Standard Soil Colour Chart. As the determination of human-made soils (previously called 'man-made soils'; Allaby, 2008; Groenman-van Waatering & Robinson, 1988) is more precise in the French soil classification system, the naming of horizons in each unit and soil classification follows the *Référentiel Pédologique* (RP, Baize & Girard, 2009). The equivalence with the World Reference Base (WRB, 2015) is specified when possible.

Selected chemical and physical analyses (Tables 3 and 4) were conducted on air-dried sieved earth fractions (2 mm). Iron (Fe_{ox}) and aluminium (Al_{ox}) were extracted using ammonium oxalate, following the 'Tamm method' (Baize, 2000), and analysed by inductively coupled plasma mass spectrometry (Thermo iCap TQ ICP-MS) at the LIEC laboratory (University of Lorraine, France). Soil pH_{water} (LAS-SOL-0501) and pH_{KCl1N} (LAS-SOL-0503) solution, cation exchange capacity (LAS-SOL-0710), exchangeable elements (LAS-SOL-0728), total carbon and nitrogen contents (LAS-SOL-0406), organic matter (OM) in soil content (calculated from organic carbon-LAS-SOL-0402-multiplied by a factor of 1.72) and grain size (LAS-SOL-0302) were measured at the soil analysis department of INRA*e* (ARRAS, France; INRA*e*, 2022).

Thin sections (9 × 6 cm) were made from undisturbed blocks (Beckmann, 1997; Murphy, 1986) at the Beckmann Laboratory (Germany). Micromorphological description (Tables 1 and 2) follows international terminology (Bullock et al., 1985; Verrecchia & Trombino, 2021), and interpretation is based on the most recent literature (Macphail & Goldberg, 2017; Nicosia & Stoops, 2017; Stoops et al., 2018). The most representative pedofeatures are illustrated in Figure 4.

PAC was performed on the Cham6 site (Figures 5 and 6) after freeze-drying and grinding soils (<250 µm). Approximately 2 g were extracted using an accelerated solvent extractor (ASE 350,

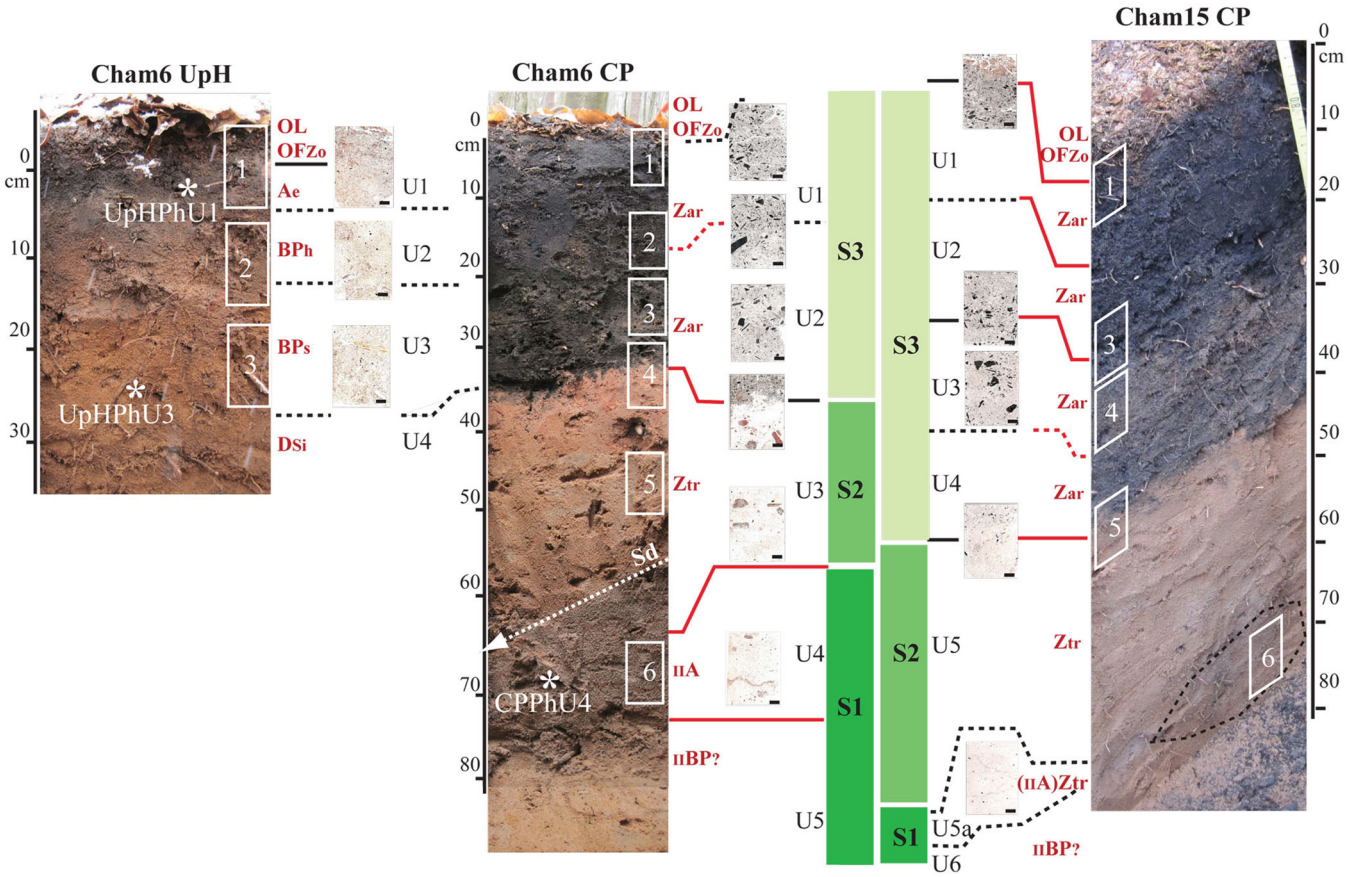

FIGURE 3 Cham6 and Cham15 profiles with the location of the thin sections. U (1,2,3,4,5): units sampled and described in Tables 1 and 2. White stars (UpH/CP-PhU1,2,4): phytolith sampling location. White rectangles: undisturbed block location/thin section. $_{II}$A, buried organomineral horizon; $_{II}$BP, buried supposed podzolic horizon; BP_h, humiferous podzolic horizon; BP_s, podzolic horizon with sesquioxydes; CP, charcoal platform profile; D_{Si}, sandy slope deposit; OF_{Zo}, organic zoogenic horizon; OL, litter; S1, ancient soil sequence; S2, platform construction sequence; S3, charred remains of charcoal production; Sd, declivity of the slope; UpH, uphill reference profile; Z_{ar}, horizon formed by anthropogenic charred debris accumulation; Z_{tr}, horizon formed by anthropogenic accumulation of geologic or pedologic origin material.

Dionex) with dichloromethane (130°C, 100 bars, 10 min, two extraction cycles). Extracts were adjusted to 5 mL in volumetric flasks. A 1 mL-aliquot was extracted. Then a surrogate PAH standard mix was added for fractionation of the extract into aliphatic hydrocarbons, aromatic hydrocarbons and polar compounds using an automated solid phase extraction on a combined cyano-bonded silica and silica phase column (ASPEC GX274; Gilson). Aromatic and polar fractions were pooled into one fraction, and an internal PAH standard mix was added. The whole sample was finally evaporated under a gentle nitrogen flow and derivatised by adding 100 µL of a mix of N,O-Bis (trimethylsilyl)trifluoroacetamide and dichloromethane (1:1; vol/vol) before heating to 60°C for 30 min. PAC quantification was performed by gas chromatography–mass spectrometry (Abuhelou et al., 2017; Biache et al., 2021).

Phytolith analysis combined phytolith extraction (see online Supporting Information Material: phytolith extraction) and soil thin section observations (Figure 8) following Vrydaghs and Devos (2018). A minimum of 100 phytoliths were counted per slide and per thin section. Observations were conducted at magnifications of ×200, ×320, ×500 and ×800 under plain polarised light and cross-polarised light. Additional observations were made under ultraviolet and blue light for differentiating heated plant materials (Devos et al., 2021). The naming of phytoliths follows ICPN 2.0 (ICPT, Neumann et al., 2019), whereas the description of their preservation is in accordance with Vrydaghs and Devos (2020).

There have been several attempts at identifying charcoal along a profile (Goldberg et al., 1994; Macphail et al., 1997) or quantifying charcoal along a profile (Bortolini et al., 2022; Gebhardt, 1991). Here, we combine quantitative and qualitative analyses on thin sections. If standard macrocharcoal analyses are carried out according to a volume unit and three-dimensional (3D) observations (Gocel-Chalté et al., 2020; Robin et al., 2014), on thin sections, only 2D surface observations are possible. The qualitative analysis of clearly recognisable charcoal fragments was carried out by measuring the surface of the charcoal per surface unit on a digitised picture from each thin section using the

TABLE 1 Field and micromorphological description of the Cham6 uphill (UpH) reference profile.

Depth (cm) unit	Field and macroscopical description	Micromorphological description
CHAM6 Uphill (UpH)		
OL	Accumulation of nonfragmented dry leaves and woody debris.	*Not sampled*.
0/+3 OF_{Zo}	Accumulation of very fragmented leaves debris. *Diffuse structural limit*.	*Mic1 very top*: Packing voids between the vegetal fragments. Dominant clear brown loose accumulation of vegetal fragments (twigs, leaves, needles, seeds, …). Very rare quartz and quartzite grains (1%). Some brown ovoid to irregular pellets (25/50 µm). Monic to enaulic groundmass.
0/−5 U1	Dark greyish to brown (2.5 YR 2/1) organic sand, structure noncrumby single grain structure, washed quartz sand grains, strongly bioturbated, numerous roots. *Diffuse colour limit*	*Mic1 top:* Packing voids between mineral grains, pellets and some fragmented vegetal elements. Loose accumulation of very small numerous brown ovoid irregular pellets (25 µm) and some vegetal fragments (aerial and roots). Some quartz and quartzite grains (20%), washed. Monic to enaulic groundmass. Mainly grass phytoliths, physically altered, isolated and rare cluster: ACUTE BULOBOSUS, ELONGATE ENTIRE, TRAPEZOID.
−5/−10 U2	Organic grey sand (2.5 YR 2/2), with darker patches, washed sand grains, angular sandstone gravels and cobbles, bioturbations (roots) more important. *Diffuse colour limit*.	*Mic1bottom, Mic2:* Packing voids between mineral grains and pellets. Quartz and quartzite sand dominant. Rounded big (500 µm, 20%) and subangular small (50–250 µm, 10%) grains. Enaulic to chitonic groundmass. Rare irregular porphyritic units (0.5 mm). Some roots and fresh more fragmented vegetal (aerial), sclerotia. Numerous small dark brown ovoid nonbirefringent units (100 µm) more or less aggregated. Rare very thin dark isotropic coating around mineral grains at the base. Small fragmented partially burned noncoated charcoal fragments, rare charcoals coated by a slightly birefringent thin cover. Rare isolated phytoliths: ELONGATE ENTIRE.
−10/−28 U3	Light brown sand (2.5 YR 6/2), angular sandstone gravels, numerous big roots. *Diffuse textural limit*.	*Mic3*: Packing voids between mineral grains. Quartz and quartzite sand dominant. Rounded big (500 µm, 20%) and subangular small (50–300 µm, 10%) grains. Some sandstone fragments (0.5–2 cm, 2%). Gefuric to locally porphyritic slightly birefringent groundmass. Some fresh vegetal fragments (mainly roots). Local accumulations of small clear brown ovoid units (50 µm) giving a fluffy structure. Brown-yellowish slightly birefringent and quite thick slightly birefringent silt coating around mineral grains and charcoals. Rare grass isolated phytoliths (1 cluster): ELONGATE ENTIRE, BLOCKY. More altered low visibility (partly covered or surrounded). Some amoebas test.
−28/−40 U4	Strong reddish-orange sand, angular sandstone cobbles and blocs, numerous big roots. *Limit of the pit*.	*Not sampled*.

ImageJ software. Only the bright-black fragments, clearly showing visible wood anatomical structures (i.e., rays, vessels, etc.) permitting identification of taxonomical types were considered as macrocharcoal. The minimum size for charcoal determination was almost 1 mm. Charcoal fragments were quantified (Figure 9) in number (#) per unit of surface (cm^2) following the pollen analysis process used by Tinner and Hu (2003) and Mooney and Tinner (2011). Depending on the visible side and state of the fragment and on the anatomy of the taxon itself, a determination may reach the genus level in some cases (e.g., *Quercus*). This approach is complementary to the classical charcoal analysis.

TABLE 2 Field and micromorphological description of the Cham6 and Cham15 charcoal platform profiles.

Depth (cm) unit	Field description	Micromorphological description
CHAM6 charcoal platform		
OL	Accumulation of nonfragmented dry leaves and woody debris.	*Not sampled*
0/+5 OF_{Zo}	Accumulation of very fragmented leaves debris. *Diffuse structural limit*.	*Not sampled*.
0/−10 U1	Thick dark greyish sand (2.5 YR 2/1), very few small rounded aggregates (0.1–0.5 cm, 80%), washed quartz grains, very few bioturbation traces, small organic remains fragments (leaves, twigs), charcoal fragments, some fine roots. *Diffuse colour limit*.	*MicF1/MicF2ht*: Packing voids between mineral grains. Quartz and quartzite sand dominant. Rounded big (500 µm, 20%) and subangular small (50–250 µm, 10%) grains. Sandstone fragments (2%). Monic to chitonic blackish groundmass. Some undefined fresh vegetal fragments, many sclerotium, fresh roots. Very rare phytoliths ELONGATE ENTIRE, isolated, one cluster. Blackish ovoid irregular faecal pellets (25/50 µm). Many fragmented big angular charcoals (deciduous trees; 20/50 µm,10%; 50/250 µm, 20%). Very abundant microfragmented charcoal (500 µm/1 cm, 10%). Around some mineral grains, very thin dark brown nonbirefringent coating.
−10/−30 U2	Thick dark greyish brown organic sand (2.5 YR 2/2) with light brown patches (2.5 YR 6/4), washed quartz grains, a few vertical biogalleries galleries and a little bit more fine roots. *Sharp colour limit following biogaleries*.	*MicF2basMic3/MicF4ht*: Packing voids between mineral grains. Quartz and quartzite sand dominant. Rounded big (500 µm, 20%) and subangular small (50–250 µm, 10%) grains. Big sandstone fragments (2%) at the bottom. Monic to chitonic blackish to brown groundmass. Rare fresh undefined vegetal fragments and decayed/altered pieces, some fresh roots. Scarce blackish to brown faecal pellets. Many fragmented big angular charcoals (deciduous trees; 20/50 µm,10%; 50/250 µm, 20%). Less abundant micro-fragmented charcoal (500 µm/1 cm, 5%). Very rare phytoliths ELONGATE ENTIRE, isolated, one cluster. Thicker dark brown nonbirefringent coatings around the mineral grains.
−30/−55 U3	Dull orange (5 YR 7/4--) sand with some light brown (2.5 YR 6/4) patches, rare gravel and some big sandstone pebbles (5–20 cm), 5%) at the base, some big roots, no biogalleries. *Sharp colour limit showing*.	*MicF4bs/MicF5*: Packing voids between mineral grains. Quartz and quartzite sand dominant. Rounded big (500 µm, 20%) and subangular small (50–250 µm, 10%) grains. Numerous big sandstone fragments (0.5–2 cm, 2%). Chitonic to gefuric brown, slightly birefringent groundmass. Rare undefined decayed/altered vegetal fragments, rare fresh roots. Seldom good to moderately preserved grass phytolith: isolated and clusters including RONDEL and ELONGATE ENTIRE. No pellets. Some more or less incompletely burned charcoal fragments. Charcoal microfragment and mineral grains coated with thick birefringent clayey silt. Rare coated charcoal. Rare thin dark brown nonbirefringent coatings as in U2, around the mineral grains some thin dusty silty more light brown coating becoming thicker towards the base of U3. Dusty rounded units of sand in a porphyritic groundmass surrounded by a dusty coating.
−55/−75 U4	Greyish sand, (7.5 YR 5/3), abundant coherent small aggregates (0.2–0.5 cm, 80%). No roots, no biogaleries. Thin (1/2 mm) brown-orange clayey lamellae. *Diffuse colour and structural limit*.	*MicF6*: Packing voids between mineral grains and local vugh in the groundmass. Quartz and quartzite sand dominant. Rounded big (500 µm, 20%) and subangular small (50–250 µm, 10%) grains. Numerous big sandstone fragments with black manganic or reddish iron cement (0.5–2 cm, 5%). Gefuric to locally porphyritic brown, slightly

(Continues)

TABLE 2 (Continued)

Depth (cm) unit	Field description	Micromorphological description
		birefringent groundmass. Abundant in situ undefined decayed/altered vegetal fragments, sclerotium. Very rare ovoid clear-brown pellets (25 μm). Rare fresh charcoals. Some grasses phytoliths (5%): cluster and dominant isolated phytoliths: RONDEL, ELONGATE. Fluo and nonfluo phytoliths, articulated phytolithes: *Elongate, crenate, rondel, trapezoïd, grass silicated short cell phytolith* capping sand grains or more or less compressed by sand grain (residual grass leave featuring compaction around quartz sand grain). Charcoal microfragment and mineral grains coated with thick birefringent silt. 2/3 mm bands of birefringent layered iron/organic clay accumulation. No phytoliths in bands. Dusty rounded units of sand in a porphyritic groundmass surrounded by a dusty coating.
−75/−80 U5	Dull orange sand (2.5 YR 7/6) with small greyish-red lenses, abundant sandstone gravels and blocks, no bioturbations. *Limit of the pit*.	*Not sampled*.
CHAM15 CP		
+5/+10 OL	Accumulation of nonfragmented dry leaves and woody debris.	*Not sampled*.
0/+5 OF_{Zo}	Accumulation of very fragmented leaves debris. *Diffuse structural limit*.	*MicF1ht*: Packing voids between the vegetal fragments. Loose accumulation of clear brown vegetal fragments (twigs, leaves, needles, seeds). Some quartz and quartzite grains (1%). No groundmass (monic). Some clear brown ovoid irregular pellets (25/50 μm).
0/−10 U1	Dark greyish brown (2.5 YR 2/2), washed sand, very few subangular aggregates (0.5–1 cm), numerous fine roots and numerous big charcoal. *Diffuse texture limit*.	*MicF1bas* (MicF2 not studied): Packing voids between mineral grains. Quartz and quartzite sand dominant. Rounded big (500 μm, 20%) and subangular small (50–250 μm, 10%) grains. Sandstone fragments (2%). Monic to chitonic blackish groundmass. Some undefined fresh vegetal fragments, many sclerotium, and fresh roots. Blackish ovoid irregular pellets (25/50 μm). Many fragmented big angular charcoals (deciduous trees; 20/50 μm,10%; 50/250 μm, 20%). Very abundant microfragmented charcoal (500 μm/1 cm, 10%). Around some mineral grains, very thin dark brown nonbirefringent coating towards the bottom of the thin section. Some (broken) physically altered phytoliths: ELONGATE.
−10/−25 U2	Dark greyish brown (2.5 YR 3/1), some coherent small rounded aggregates (0.1–0.5 cm), some small roots, big charcoal fragments. *Undulated diffuse colour limit*.	*MicF3ht*: Packing voids between mineral grains. Quartz and quartzite sand dominant. Rounded big (500 μm, 20%) and subangular small (50–250 μm, 10%) grains. Big sandstone fragments (2%) at the bottom. Monic to chitonic blackish to brown groundmass. Rare fresh undefined vegetal fragments and decayed/altered pieces, some fresh roots. Blackish to dark brown ovoid pellets (25 μm). Many fragmented big angular charcoals (deciduous trees; 20/50 μm, 10%; 50/250 μm, 20%). Less abundant microfragmented charcoal (500 μm/1 cm, 5%). Thin dark brown coating around the mineral grains. Thin, more clear, brown, nonbirefringent coatings around mineral grains. Phytoliths.

TABLE 2 (Continued)

Depth (cm) unit	Field description	Micromorphological description
25/−38 U3	Greyish brown (2.5 YR 4/2), small gravels, some vegetal fragments (leaves, twigs), numerous roots, darker mottle, middle-sized charcoals. *Diffuse colour limit*.	*MicF3bs/MicF4ht*: Packing voids between mineral grains. Quartz and quartzite sand dominant. Rounded big (500 µm, 20%) and subangular small (50–250 µm, 10%) grains. Big sandstone fragments (2%) at the bottom. Monic to chitonic blackish to brown groundmass. Rare fresh undefined vegetal fragments and decayed/altered pieces, some fresh roots. Some blackish to dark-brown pellets. Less big angular charcoals (deciduous trees; 20/50 µm,10%; 50/250 µm, 20%). Abundant microfragmented charcoal (500 µm/1 cm, 5%). Dark brown coating around the mineral grains. Thin, more clear and brown coatings around mineral grains. Rare (broken) physically altered phytoliths: ELONGATE ENTIRE.
−38/−50 U4	Dark brown (2.5 YR 2/3) sand, rounded coherent aggregates (0.2–1 cm, 20%) some roots, abundant small charcoal. *Sharp strait colour limit*.	*MicF4bs/MicF5ht*: Packing voids between mineral grains. Quartz and quartzite sand dominant. Rounded big (500 µm, 20%) and subangular small (50–250 µm, 10%) grains. Big sandstone fragments (2%) at the bottom. Monic to chitonic blackish to brown groundmass. Very rare fresh undefined vegetal fragments and more abundant decayed/altered pieces, some fresh roots. Scarce blackish to brown pellets (25 µm). Abundant microfragmented charcoal (500 µm/1 cm, 5%). Rounded soil horizon fragments. Some coated small charcoals. Dark brown coating around the mineral grains. Some more birefringent clear brown coatings. Rare (broken) physically altered phytoliths: ELONGATE ENTIRE.
−50/−75 U5	Light yellowish brown (7.5 YR 6/4) sand, coherent rounded aggregates (0.5–1.5 cm), some fine roots. *Diffuse colour limit*.	*MicF5bs*: Packing voids between mineral grains. Quartz and quartzite sand dominant. Rounded big (500 µm, 20%) and subangular small (50–250 µm, 10%) grains. Numerous big sandstone fragments (0.5–2 cm, 2%). Chitonic to gefuric brown, slightly birefringent groundmass. No pellet. Some incompletely burned charcoal fragments and rare coated microfragmented charcoal. Thicker dusty silty birefringent clear brown coatings around the mineral grains. One fragment of melted silicate at the top.
−75/−85 U5a	Large more greyish brown irregular lenses (7.5 YR 5/3), abundant coherent small aggregates (0.2–0.5 cm, 80%), roots fragments. *Trench limit*.	*MicF6*: Packing voids between mineral grains and local void in the groundmass. Quartz and quartzite sand dominant. Rounded big (500 µm, 20%) and subangular small (50–250 µm, 10%) grains. Numerous big sandstone fragments with black manganic or reddish iron cement (0.5–2 cm, 5%). Gefuric to locally porphyritic brown, slightly birefringent groundmass. Abundant undefined decayed/altered vegetal fragments, sclerotium. Very rare clear brown ovoid pellets (25 µm). Microfragmented coated charcoal. Thick dusty silty birefringent brown coating around the mineral grains. 2/3 mm bands of iron/organic birefringent clay accumulation. Unconnected phytoliths (5%): some BLOCKY, many ELONGATE.
−85/−90 U6	Yellowish brown (7.5 YR 5/6), abundant coherent rounded aggregates (0.5–1 cm, 60%), rare fragmented roots. *Deepness checked by drill/core*.	*Not sampled*.

TABLE 3 Soil analytic data and grain size analysis from the Cham6 profile.

Cham6	Depth (cm)	pH_{water}	C_{tot} (%)	N_{tot} (%)	C/N	Ca^{++} exchangeable cmol(+)/kg	OM (%)	Grain size (%)					Hz
								CS	FS	CL	FL	C	
UpH													
U1	0/−5	4.5	3.39	0.13	26.1	0.13	5.86	60.7	24.3	2.7	8.0	4.3	A_e
U2	−5/−10	4.2	1.78	0.05	35.6	0.05	3.09	62.1	25.0	1.9	5.5	5.5	BP_h
U3	−10/−28	4.9	1.32	0.04	33	0.02	2.28	64.2	22.4	3.1	5.3	4.3	BP_s
U4	−28/−40	4.9	0.97	0.03	32.3	0.03	1.68	64.9	24	2.2	4.7	4.2	D_{Si}
CP													
U1	0/−10	4.24	6.21	0.19	32.9	0.39	10.75	53.3	34.9	3.2	4.7	3.9	Z_{ar}
U2	−10/−30	5.36	2.98	0.07	42.6	3.68	5.16	51.7	39.3	2.5	3.2	3.3	Z_{ar}
U3	−30/−55	5.87	0.37	0.006	61.7	0.62	0.64	61	29.8	2.2	3.5	3.5	Z_{tr}
U4	−55/−75	5.92	*0.65*	0.002	*325*	0.70	*1.12*	66.2	29.2	2.4	3.9	2.3	$_{II}A$
U5	−75/−80	6.21	0.44	0.005	87.8	0.97	0.76	51.3	37.1	3.1	4.0	4.5	$_{II}BP$?

Abbreviations: C, clay; Ca++ (cmol/kg), calcium; CL, coarse loam; CP, charcoal platform; CS, coarse sand; FL, fine loam; FS, fine sand; Hz, horizon name; OM (%), organic matter; *N*(%), total nitrogen; pH_{water}, C_{tot}(%), total carbon; UpH, uphill.

TABLE 4 Table of Tamm analytic data (Al_{ox}–Fe_{ox} µg/g) from Cham6 and Cham15 profiles.

	Depth (cm)	Tamm		Colour code	Hz
		Al_{ox} (µg/g)	Fe_{ox} (µg/g)		
Cham6					
UpH					
U1	0/−5	668.5	856.1	2.5 YR 2/1	A_e
U2	−5/−10	1507.3	1439.2	2.5 YR 2/2	BP_h
U3	−10/−28	3434.2	1872.9	2.5 YR 6/2	BP_s
U4	−28/−40	/	/	2.5 YR 6/7	D_{Si}
CP					
U1	0/−10	1303.2	1198.1	2.5 YR 2/1	Z_{ar}
U2	−10/−30	1306.7	922.7	2.5 YR 2/2 (6/4 patches)	Z_{ar}
U3	−30/−55	720.2	498.8	2.5 YR 6/4	Ztr
U4	−55/−75	287.2	291.6	2.5 YR 6/6	$_{II}A$
U5	−75/−80	/	/	2.5 YR 7/6	$_{II}BP$?
Cham15					
CP					
U1	0/−10	1249.0	1149.7	2.5 YR 2/2	Z_{ar}
U2	−10/−25	1608.0	1176.4	2.5 YR 3/1	Z_{ar}
U3	−25/−38	1257.5	969.7	2.5 YR 4/2	Z_{ar}
U4	−38/−50	1239.8	856.2	2.5 YR 2/3	Z_{tr}
U5	−50/−75	1025.0	756.0	7.5 YR 6/4	Z_{tr}
U5a	−75/−85	472.3	460.0	7.5 YR 5/3	$(_{II}A)Z_{tr}$
U6	−85/−90	*513.3*	386.8	7.5 YR 5/6	$_{II}BP$?

Abbreviations: CP, charcoal platform; Hz, horizon name; UpH, uphill.

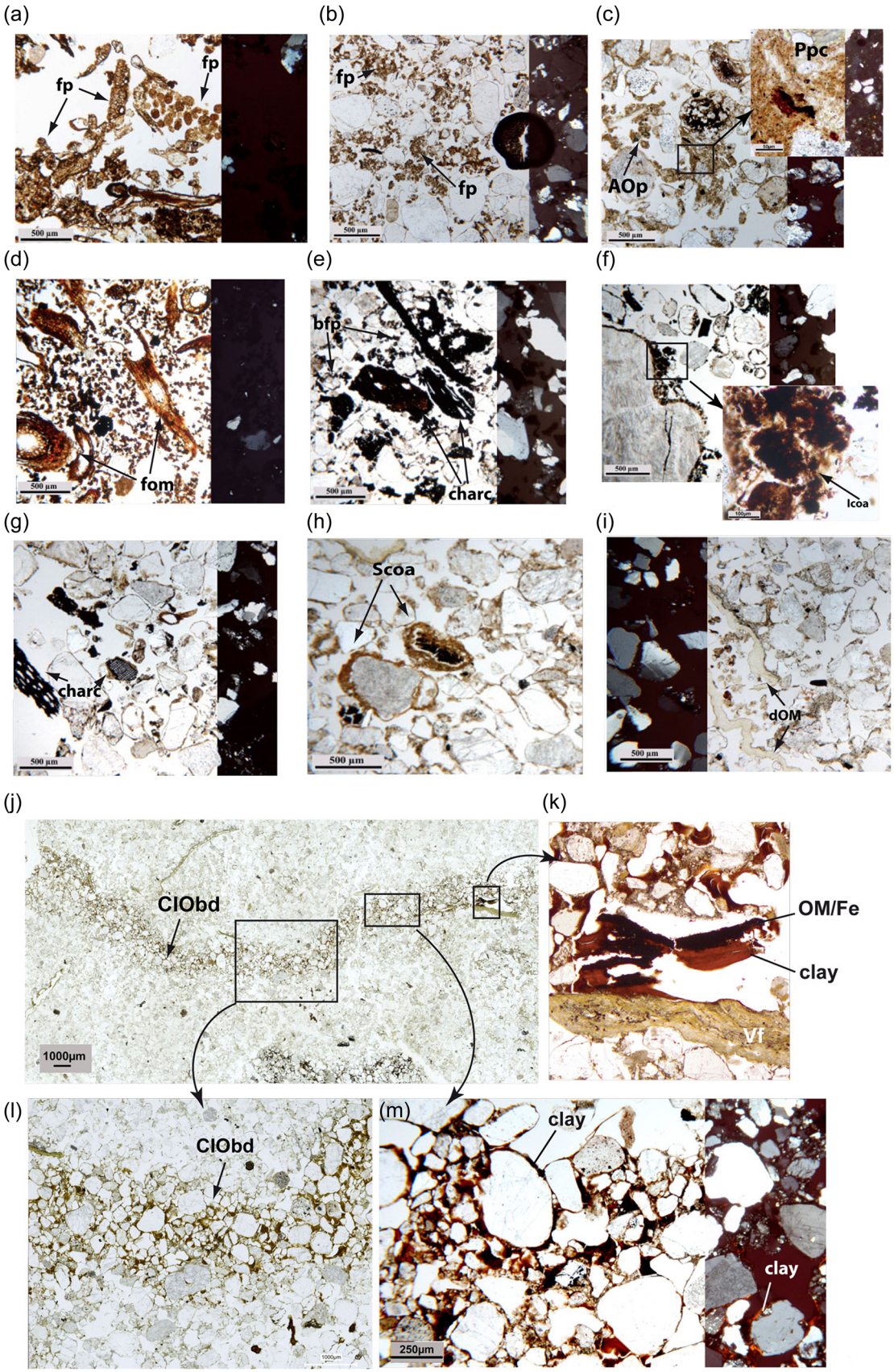

FIGURE 4 (See caption on next page).

3 | RESULTS

3.1 | Pedosedimentary analysis of the sequences

3.1.1 | The UpH reference soil

The UpH reference profile dug outside the CP comprises four units separated by diffuse limits (Figure 3). A thin organic litter unit OL covers a dark-greyish-to-brown thin organic fragmented zoogenic OFZo level (Figure 4a). The transition with the lower noncrumby but pellety U1 unit is gradual.

U1 is characterised by a microscopic loose accumulation of dark-brown ovoid isotropic organic faecal dejections from small invertebrate mesofauna (Figure 4b) and small plant fragments. Partially aggregated OM includes rare fine mineral fractions. Groundmass shows an enaulic-related distribution (Righi & Lorphelin, 1987). Coatings around sand grains are absent. The amounts of measured Fe_{ox} and Al_{ox} are low (Table 4).

In the U2 and U3 levels, thin dark-reddish-brown isotropic pellicular coatings and fluffy structured OM formed of partially aggregated, brown, 100-µm-large smooth isotropic ovoids (Figure 4c) reveal a polymorphic microfabric. Slightly birefringent silty-clay coatings wrap small charcoal fragments and some mineral grains. Concentrations of Fe_{ox} and Al_{ox} increase (Table 4). The C/N ratio is between 25 and 45 (Table 3).

U4 is a coarse reddish-orange sand (>85% sand; Table 3) with angular fragments of sandstone gravel and cobbles, not sampled for thin section analysis.

3.1.2 | The Cham6 and Cham15 CP sequences

The organic noncrumby OF_{zo} layer (Figure 4d) is rich in faecal pellets and covers two dark units (U1 and U2 in both Cham6 and Cham15). They show fresh, partially decayed and fragmented charred plant residues. U2 is similar to U1 but shows a more coherent macro-structure, still with very few aggregates and smaller blackish to dark-brown ovoid micropellets. Less abundant microscopic charcoals are microfragmented.

In Cham6, U1 total carbon (C_{tot}) and OM concentrations are twice as high (6.2% and 10.75%, respectively; Table 3) as in the UpH profile. Thin section observations show many well-preserved, nonoriented angular charcoal fragments (Figure 4e) throughout all these units. A large proportion of 0.5–2 cm fragments were identified as charred deciduous wood. The large and fresh charcoal fragments in these upper dark layers show no evident refitting characteristics. Some appear to be more or less well carbonised (with, respectively, black or reddish faces in reflected light). Their vessels are devoid of any mineral or organic infill. In the U2 lower unit, charcoal seems more finely fragmented, and the quantities of small blackish ovoid irregular mites and enchytraeids dejections (Babel, 1975) decrease. Black faecal pellets are abundant (Figure 4e), and the matrix is sparse between the coarse rounded quartz grains and sandstone fragments. In the whole Cham6 profile, very thin nonbirefringent dark-black to brownish quartz grain coatings are observed (Figure 4f). Exchangeable calcium concentrations (Ca^{2+}) are very low, except for a peak in U2 (3.68 cmol/kg vs. less than one in units above and below; Table 3). Crystallised pseudomorphosis of calcium oxalate (ash) was not observed in thin sections.

At Cham15, the upper dark charcoal residue layers U1/U2 overlie a 20 cm thick greyer subsequence formed by U3 and U4. On the profile, the top of U4 is rich in 1–5-cm-large decayed roots, producing local brownish patches (U4). The boundary between U2 and U3 is gradual. Microscopic, fragmented small charcoals dominate the less abundant fine charcoal dust, giving this layer its paler greyish colour with less numerous blackish faecal pellets (Figure 4g). As for Cham6, no crystallised ash carbonates are observed in thin sections.

A 25–30-cm-thick reddish sandy level underlies the Cham6 and Cham15 charcoal residual deposits (respectively U3 and U5; Figure 3). Stones are rare, except for an isolated blunt-edged boulder at the base of the Cham6 profile. The microscopical groundmass is absent, and the mineral compound (quartz grains and sandstone fragments) is loose (Figure 4g). As in the modern reference soil profile, some very small charcoal pieces are coated with slightly birefringent silt (Figure 4h). Vegetal elements are rare. Except for relatively deep large root concentrations, no microscopic faecal dejections, faunal galleries or chambers were observed. The limits (Figure 3) between the charcoal residual deposits and this reddish unit are extremely sharp, even at the microscopic scale.

In Cham6, at a depth of about 70 cm, the platform layer (U3) covers a thick light-grey U4 level (Figure 3), following the natural slope. At Cham15, a similar grey unit (U5a; Figure 3) shows irregular clumps traversed by large roots in places. Microscopically, both levels show a more porphyritic and slightly birefringent groundmass. Small dark-brown irregular ovoid faunal dejections and non-birefringent decayed pale vegetal residues (Figure 4i) were observed. In U5/Cham15, these vegetal fragments appear disturbed in the clods but nonetheless seem to be in

FIGURE 4 Some representative micromorphological pedofeatures. *Current reference Cham6 UpH profile*. (a) OF_{Zo} organic horizon with many fresh vegetal fragments and faecal pellets (fp). (b) $U1/A_e$ organomineral horizon with washed sand grains and numerous fp. (c) $U3/BP_s$ podzolic horizon with aggregated ovoid pellets (Aop) and pellicular polymorphic coatings (Ppc). *Charcoal platform*. (d) Cham15: OF_{zo} very organic horizon with fresh organic matter (fom) and many fp. (e) Cham6: $U1/Z_{ar}$ dark horizon with numerous charcoal fragments (charc) and blackish faecal pellets (bfp). (f) Cham6: $U2/Z_{ar}$ dark horizon with reddish iron coating (Icoa) around quartz sand grains; (g) Cham15: $U3/Z_{ar}$ greyish horizon with rare fps, medium-sized charcoal fragments (charc) and relatively washed quartz grains. (h) Cham6: $U3/Z_{tr}$ platform sediment with slightly birefringent silt coatings (Scoa) around quartz grains and ancient charcoal. (i) Cham15: $U5a/(_{II}A)Z_{tr}$ clods of buried organomineral horizon with decayed vegetal fragments (dOM). (j) Cham6: $U4/_{II}A$, general view of a clayey iron organic band (ClObd). (k) Cham6: $U4/_{II}A$, detail of iron (Fe)/organic (OM) and clay accumulations, note the decayed vegetal fragments (Vf). (l, m) Cham6: $U4/_{II}A$, details of the clayey iron organic band (ClObd) with birefringent clay accumulations (clay).

situ and are more or less parallel to the slope in U4/Cham6. In U4, total carbon and OM concentrations are slightly higher (Table 4) compared to the upper (U3) and underlying (U5) layers.

At the top of the grey unit (at a depth of 0.60–0.75 cm) under both the Cham6 and Cham15 platforms, many small, thin brown-reddish bands (0.5 cm thick, 5 cm long) were observed parallel to the horizontal CP surface. Under the microscope, these slightly birefringent fine layers (Figure 4j,l,m) look like iron/organic deposits overlying reddish ferruginous clay deposits (Figure 4k). This was not highlighted by grain size analysis as the clay content of U4 (Cham6) is lower than in the current U1 horizon from UpH (Table 3). No phytoliths or fine charcoals were observed in these bands.

At the bottom of both profiles, units U5 (for Cham6) and U6 (for Cham15) are composed of coarse reddish-orange sand, macroscopically very similar to the U3 substrate deposit UpH.

Values of pH_{water} are more alkaline in comparison to the current UpH reference soil profile (<5) and increase with depth, reaching 6.21 at the base of the Cham6 profile (Table 3).

3.2 | Polycyclic aromatic compounds

3.2.1 | The current UpH reference soil

The UpH reference soil contains rather moderate PAH concentrations (Figure 5) ranging from 0.02 to 1.2 µg g^{-1}, which decrease the profile from U1 to U3. The PAC distributions (Figure 6) are characterised by the predominance of intermediate- to heavy-molecular-weight PAHs containing 4–6 rings. Such concentrations and distributions are classically observed in forest soils (Bucheli et al., 2004; Plachá et al., 2009) and are characteristic of the regional incomplete combustion of coal, wood or grass. They are associated with particulate matter emitted in the atmosphere and are transported over long distances before they are deposited on the soil surface.

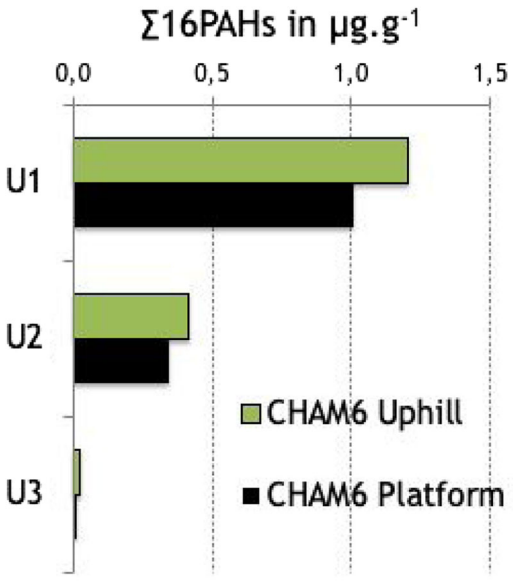

FIGURE 5 Sum of the 16 Environment Protection Agency PAHs in the three levels (U1, U2 and U3) of CHAM6 UpH (green bars) and platform (black bars) soils in µg g^{-1}. PAH, polycyclic aromatic hydrocarbon.

3.2.2 | The Cham6 CP sequence

The Cham6 CP soils present the same PAH concentrations (0.01–1.01 µg g^{-1}) as the UpH soils and a similar decrease from

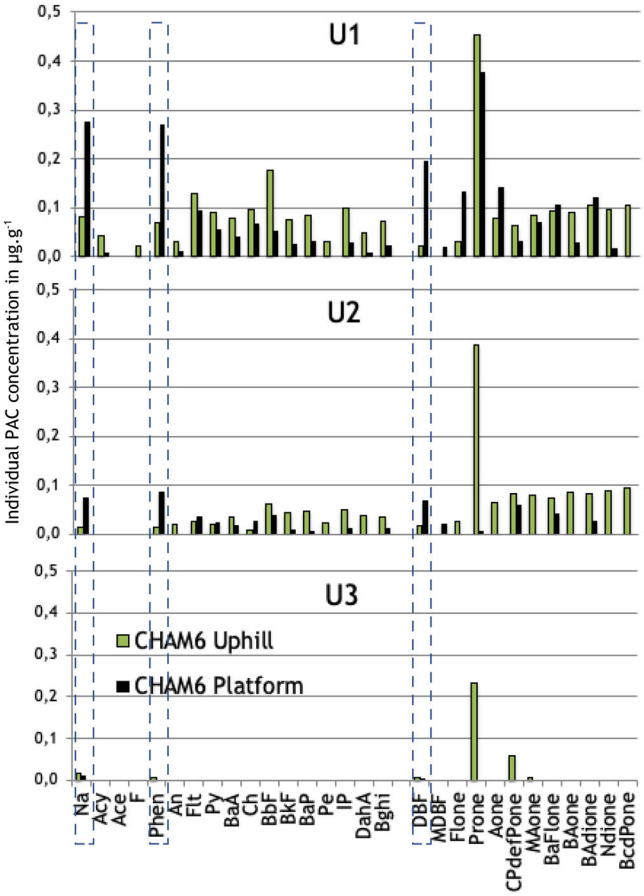

FIGURE 6 Concentrations in µg g^{-1} of 29 individual PACs quantified in the three levels (U1, U2, U3) of CHAM6 UpH (green bars) and platform soils (black bars). Ace, acenaphthene; Acy, acenaphthylene; Ant, anthracene; Aone, anthraquinone; BaA, benzo[*a*]anthracene; BAdione, benzoanthracenedione; BaFone, benzo[*a*]fluorenone; BAone, benzanthrone; BaP, benzo[*a*]pyrene; BbF, benzo[*b*]fluoranthene; BcdPone, benzo[*cd*]pyrenone; Bghi, benzo[*ghi*]perylene; BkF, benzo[*k*]fluoranthene; Ch, chrysene; CPdefPone, cyclopenta[*def*]phenanthrone; DahA, dibenzo[*ah*]anthracene; DBF, dibenzofuran; F, fluorene; Flone, 9*H*-fluorenone; Flt, fluoranthene; IP, indeno[1,2,3-*cd*]pyrene; MAone, methylanthracene-9,10-dione; MDBF, 4-methyldibenzofuran; Nap, naphthalene; Ndione, naphtacene-5,12-dione; PAC, polycyclic aromatic compound; Pe, perylene; Phe, phenanthrene; Prone, perinaphtenone; Py, pyrene.

U1 to U3 (Figure 5). However, PAC distributions are significantly different from those in the UpH soils (Figure 6). They are dominated by two low-molecular-weight PAHs, naphthalene and phenanthrene. High-molecular-weight PAHs are poorly represented compared to the UpH soils. Dibenzofuran also appears as an oxygenated PAC specific to CP soils. Despite the decrease in PAC abundance with depth, this characteristic charcoal-making activity distribution persists in U2 but could not be detected in U3.

3.3 | Phytolith analysis in bulk samples and thin sections

3.3.1 | The current UpH reference soil

Grassy and nongrassy phytoliths characterise the assemblage extracted from the UpH reference soil (UpHPhU1). RONDEL (Figure 8a) dominates the grass record, which also includes TRAPEZOID, ACUTE and ELONGATE ENTIRE. The additional BLOCKY (Figure 8b), POLYHEDRAL and UNKNOWN are understood as nongrassy phytoliths (Figure 7b). In thin sections, phytoliths are mainly distributed as isolates with some clusters.

With UpHPhU3, the presence of morphologically unidentifiable phytoliths as well as fragments is more marked (Figure 7a). Grass phytoliths outnumber the identifiable ones, with a clear prevalence of RONDEL. Thin sections show that all phytoliths are distributed in the polymorphic groundmass surrounding the sand grain (Figure 8c), mainly as isolates. Some autofluorescent phytoliths, as well as melted ones, are also observed. In thin sections, the observation of amoeba (Figure 8d) and diatom (Figure 8e) out of the groundmass is noteworthy.

3.3.2 | The Cham6 CP sequence

The very rare phytoliths observed in the dark charcoal layers (U1/U2) are all isolated and clustered. While the observed clusters mainly comprise fragments, the isolated ones are ELONGATE ENTIRE.

In unit U3, rare grass phytoliths (RONDEL and ELONGATE ENTIRE) are well to moderately preserved. They are mainly isolated and clustered.

The CPPhU4 (Figure 3) phytolith assemblage shows marked similarities with UpHPhU1 (Figure 7b). However, in CPPhU4, phytolith types such as BLOCKY, POLYHEDRAL and UNKNOWN are less frequent, while BILOBATE and TRAPEZIFORM become more frequent. We observe a general trend towards more morphologically diverse grass phytoliths. Clustered phytoliths are twice as frequent. Coloured, melted opal (Figure 8g) and fluorescent (Figure 8h) grass and nongrass phytoliths also occur at this level. In the U4 thin section, fluorescent and nonfluorescent phytoliths are mostly isolated and derive mainly from grasses (RONDEL, ELONGATE ENTIRE). They appear to be disarticulated and mostly physically altered (Figure 8i). There are no phytoliths in the bands. Specific phytolith features, capping or more or less compressed between sand grains (Figure 8j–l), are observed in the upper half level of U4. They are exclusively composed of grass phytoliths (ELONGATE, CRENATE, RONDEL, TRAPEZOID and grass silica short cell phytolith).

3.4 | Macrocharcoal observations

Out of a total of 346 charcoal pieces (256 on Cham6 and 90 on Cham15), the taxonomical analysis resulted here in the identification of a minimum of two taxa for Cham15 (angiosperm and *Quercus*) and a maximum of five taxa for Cham6 (angiosperm, *Quercus*, *Fagus*, *Alnus/Betula*, *Prunus*). Nonidentifiable taxa in thin sections are grouped in the angiosperm class. No conifers were observed. The general trend in charcoal assemblage composition appears relevant in the thin section results and is consistent with the standard anthracological analysis (Gocel-Chalté et al., 2020).

On both Cham6 and Cham15, charcoal concentrations are much richer in the upper residual sequence (S3) compared to the S2/S1 sequences below (Figure 9a,b). This is very clear on Cham6 (Figure 9a), with a sharp difference in charcoal concentration between the charcoal-hearth layers (S3) and the underlying platform (S2). On Cham15, a sharp decrease in charcoal concentration appears at U4 (Figure 9b). In relative values, the observation of S3 on both sites (Figure 9c,d) points to a rather similar taxonomical spectrum. *Fagus* is observed in all Cham6 sequences but is absent from Cham15. A few fragments of *Alnus/Belula* (more probably *Betula*, according to Gocel-Chalté et al. [2020]) and *Prunus* are recorded in Cham6. However, for Cham15, more abundant non-identifiable small, fragile ligneous tree twigs, grouped in the angiosperm class, imply a lower amount of identified taxa.

Further down, the charcoal taxonomical spectrum does not vary significantly in platform S2, apart from the absence of *Betula* and *Prunus* in Cham6.

In the buried S1 sequence, only nonidentifiable angiosperm charcoal was observed at Cham15.

4 | DISCUSSION

4.1 | Soil profile characterisation

4.1.1 | The current natural UpH soil profile

For the UpH profile, the thinness of the organic horizon (OL, OF_{zo}) and its gradual transition towards the lower U1 noncrumby horizon define a *hemimoder* humus type (Jabiol et al., 2009).

As seen in the results section, the micromorphological characteristics and the small amounts of measured iron and aluminium from U1 indicate the initial mobilisation of chelates (soluble organomineral complexes) towards the base. Based on this assumption, U1 was interpreted as an eluvial Ae horizon.

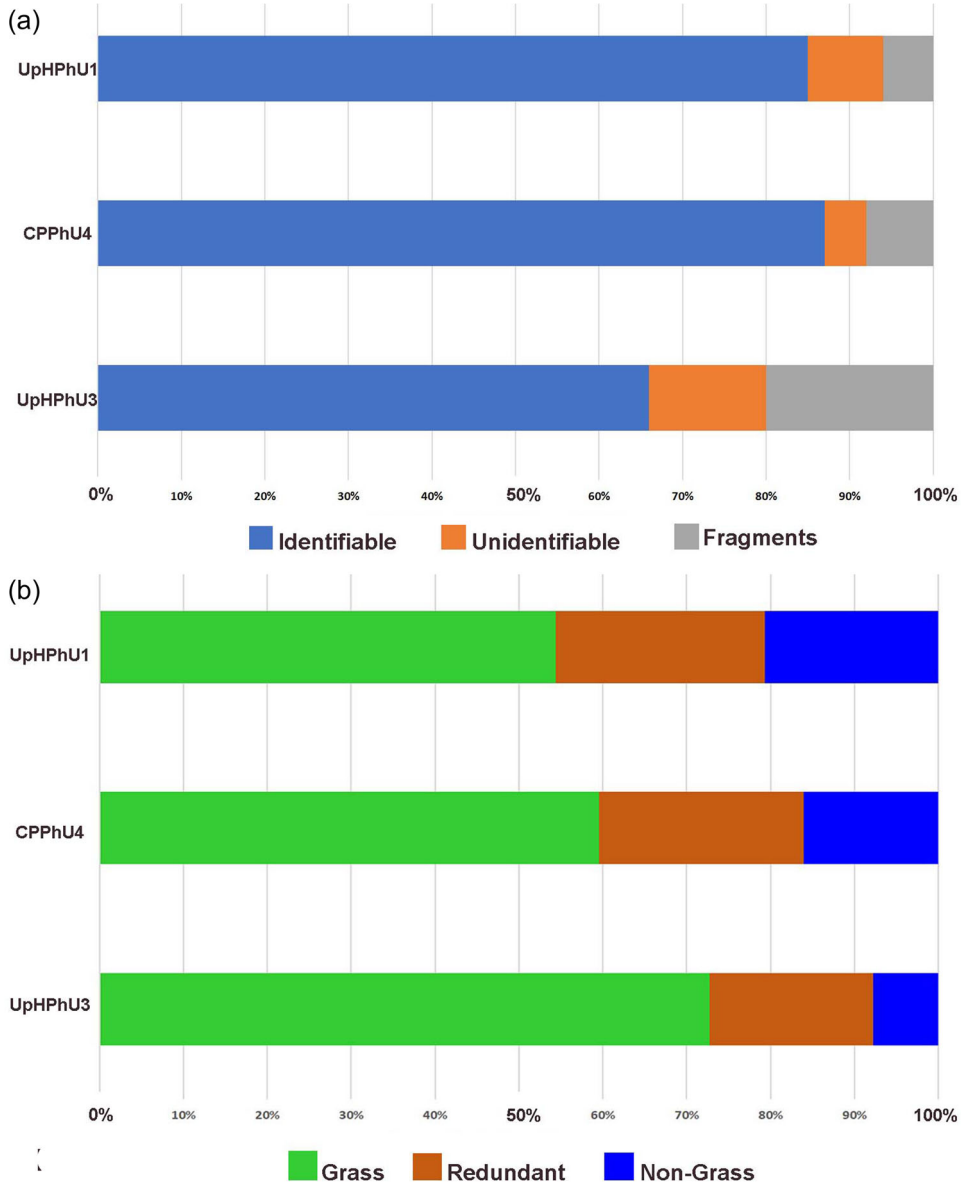

FIGURE 7 (a) Relative frequencies of morphologically identifiable phytoliths (MI), unidentifiable phytoliths (UI) and fragments observed after extraction. UpHPhU1/UpHPhU3 phytolith samples in the UpH reference soil, CPPhU4 phytolith sample in the palaeosol under the charcoal platform. (b) Simplified phytolith assemblages. All the observed phytoliths are distributed in three categories; grass phytoliths, redundant phytoliths and nongrass phytoliths. Compared to UpHPhU1 and CPPhU4, UpHPhU3 assemblage attests to a much more marked presence of grass phytoliths. While both UpHPhU1 and CPPhU4 associated grass and nongrass phytoliths, the latter are more frequently observed with UpHPhU1 while CPPhU4 contains more frequent grass phytoliths.

Following Kemp (1985), the polymorphic microfabric may be linked to a combination of organo-Al or organo-Al/Fe complexes resulting from plant residue transformation and mixing by fauna. This usually occurs in acid conditions and can be observed in both aluminic (Sal) and podzolic (BP) horizons (Baize & Girard, 2009). Alone, this microfabric is not a good discriminant for the U2/U3 unit denomination, but considering the Al and Fe amorphous product precipitation suggested by high Al_{ox} and Fe_{ox} in these layers compared to U1, here it may characterise a podzolic horizon (spodic horizon from the WRB; De Conninck & Righi, 1981; Guillet, 1987; Legros, 2007; Van Ranst et al., 2018; Righi & Lorphelin, 1987). U2 and U3 may thus be podzolic horizons, respectively, named BP_h and BP_s.

U4 is a mainly mineral sediment layer, except for some very fine silt-coated charcoal, covering the nonweathered Triassic local sandstone. The very thin, nonbirefringent dark-black-to-brownish quartz coatings are attributed to the relict iron/manganese cement from local ferruginous Triassic sandstone. Physical weathering of the Vosgian Triassic sandstone produced a homogeneously granular sandy slope deposit that was reworked during past interglacial periods. The interglacial periods were characterised by extreme hydroclimatic conditions (snow melting

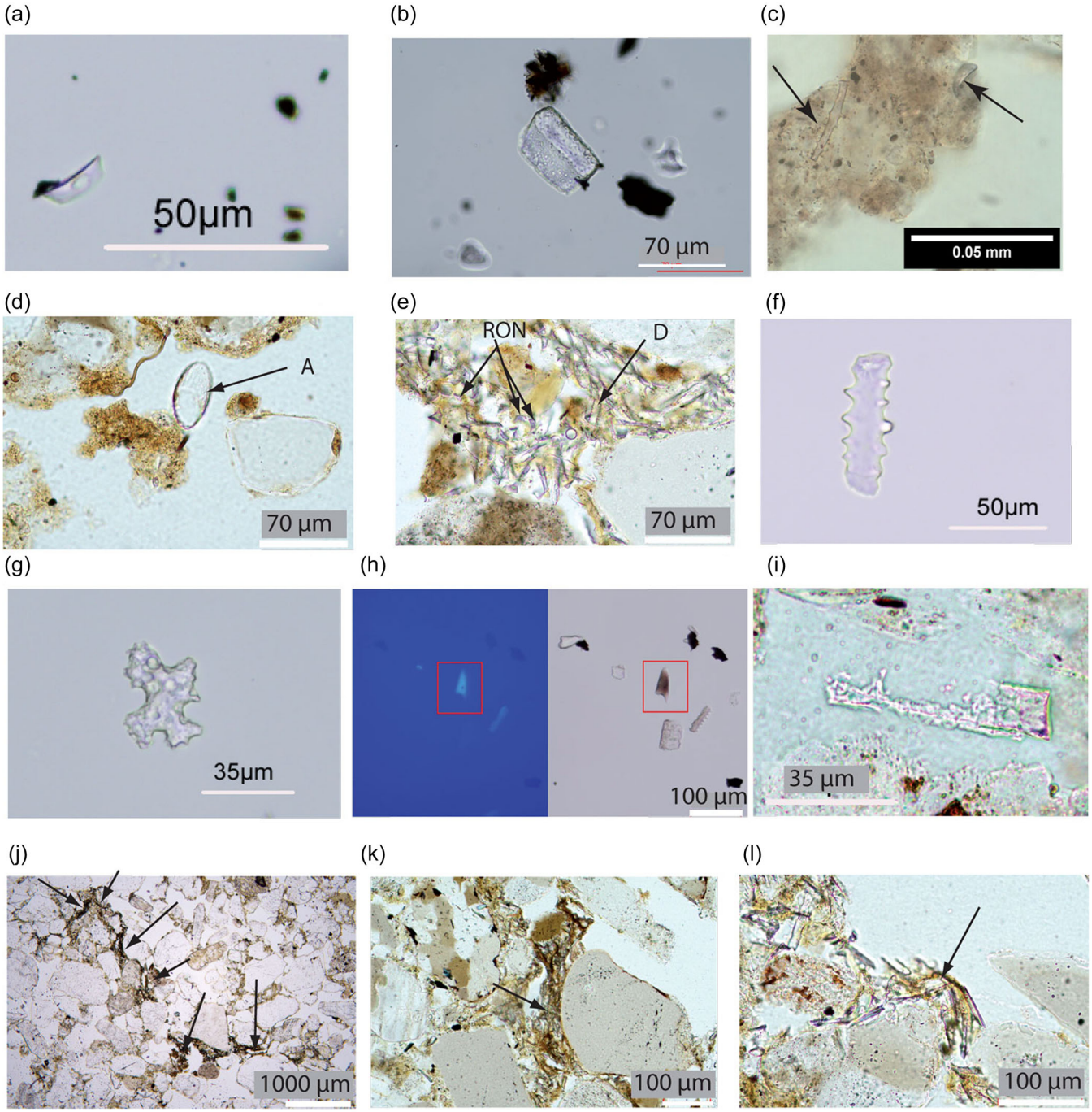

FIGURE 8 Phytoliths, amoeba test and diatom observed in the reference profile UpH and Cham6 CP. (a) RONDEL, UpHPhU1 (×500 on bulk preparation), (b) BLOCKY, UpHPhU1 (×500 on bulk preparation), (c) ELONGATE DENTATE (lefts) and RONDEL (right) in the polymorphic groundmass around sand grains, UpHU3 (PPL, ×400 on thin section). (d) Amoeba test UpH/U3 (×500 PPl on thin section). (e) Diatom (D) and RONDEL accumulation (RON) CPU4 (×500 PPL on thin section), (f) UNKNOWN CPPhU4 (×500 on bulk preparation), (g) melted phytolith, CPPhU4 (×500 on bulk preparation), (h) ACUTE BULBOSUS heated, CPPhU4 (×200 on bulk preparation) left: UV, right: PPL, (i) altered phytolith CP/U4 (×500 on thin section). (j) Accumulation of several residual grass phytoliths, featuring the deposit of a dead grass leaf in the palaeosol (U4) under the CP (×40 on thin section). (k) Detail of j showing the compaction of the leaf around the quartz sand grains (×200 on thin section). (l) Detail of j, showing phytoliths capping a quartz grain with compaction (×500 on thin section). CP, charcoal platform; PPL, plain polarised light; UV, ultraviolet.

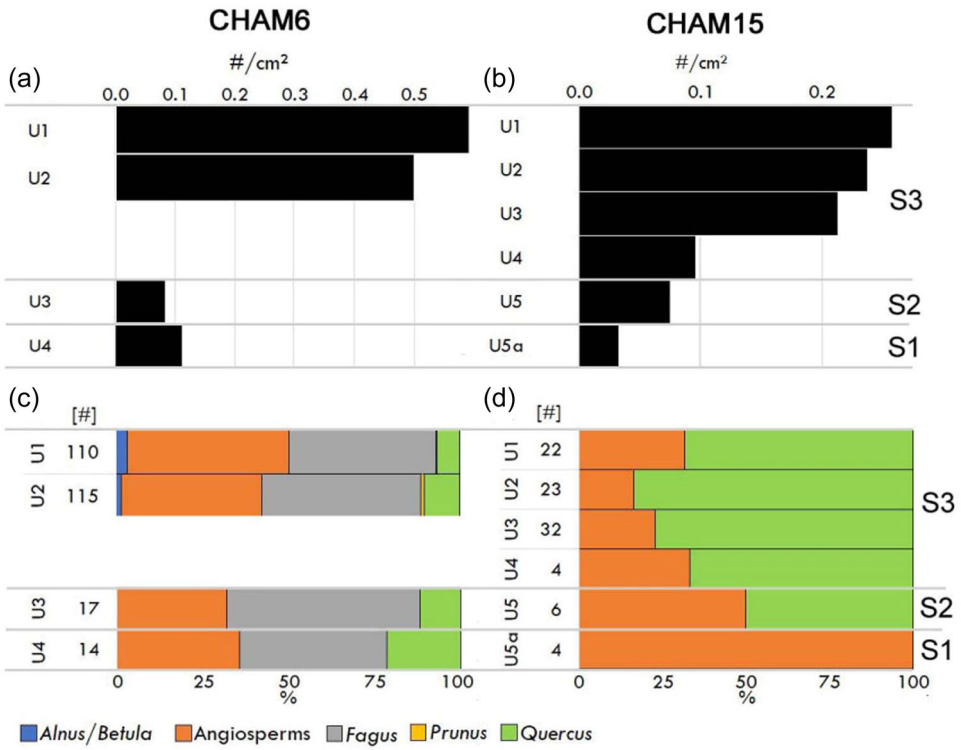

FIGURE 9 Results of the total charcoal count ([a] Cham6, [b] Cham15), and taxonomical identification per stratigraphic unit ([c] Cham6, [d] Cham15). [#], number of determined charcoals (on A/B) and number of determined taxa (on C/D); CP, charcoal platform; U, stratigraphical unit.

on ice, heavy rains after drought [Guillet et al., 1979]). Along with rare dusty rounded units, the birefringent silt coatings around grains and charcoals also observed in U2/U3 are attributed to soil mass movement (Van Vliet-Lanoë, 1998; Van Vliet-Lanoë & Fox, 2018) and confirm this interglacial or later Holocene colluviation. This coarse sandy colluvial substrate creates well-drained, very acidic edaphic conditions (pH < 5), unsuitable for biological activity, especially by anecic earthworms. This coarse and transported unit (D), fragmented from hard silicate stone (Si), is called D_{Si} horizon (Baize & Girard, 2009).

At the profile scale, the formation of a hemimoder humus and the C/N ratio of 25–45 support the existence of podzolisation processes (Baize, 2000) in this soil. On this steep slope, lateral water movement is dominant over vertical water infiltration, thus hindering the formation of a strongly developed eluvial horizon (Duchaufour, 1955). This renders the distinction of micropedofeatures unclear (Macphail, 1981).

According to field and micromorphological observations, chemical data, and following the French soil reference collection (RP), the current UpH soil dug UpH 10/15 m outside the platform Cham6 is a *podzosol ocrique* (Baize & Girard, 2009), which corresponds to the *entic podzol* of the World Reference Base (WRB, 2015). It is characterised by a *podzolic BP* horizon (spodic, WRB) without a clear upper eluvial horizon (albic, WRB) on top.

4.1.2 | The CP soil profiles (CPs Cham6 and Cham15)

Similar to the UpH profile, the relatively thin organic horizons (OL, OF_{zo}) are also defined as a *hemimoder* humus type (Jabiol et al., 2009).

In the upper charcoal accumulation units (U1/U2 for both Cham6 and Cham15), the fresh aspect with empty vessels and no evidence of charcoal residue refitting suggests a lack of fragmentation after the final combustion episode. The absence of crystallised ash in thin sections and the low concentrations of exchangeable Ca^{2+} suggest high dissolution rates in this acidic soil context, followed by rapid drainage through the CP. At Cham6, the sparse matrix between the mineral compounds, the more coherent macrostructure, and the decrease of mite and enchytraeids pellets attest to the start of weak horizon differentiation in U2 charcoal deposits. In this last unit, the exchangeable Ca^{2+} peak may relate to a residue of crystallised calcium carbonate dissolution (from ash accumulations), which is no longer observable in thin sections. At Cham15, the limit between U2 and U3 is sharp, and pedogenetic processes are underlined by more accentuated faunal mixing in the lower U3/U4 organic layers. The brutal decrease in the concentration of charcoal between U3 and U4 (Figure 9b) may indicate a change in charcoal production, the reworking of residual charcoal layers and/or differentiate the transformation of OM by mesofauna. Moreover, as they lie directly on the artificial platform, the U3/U4

lighter dark units from Cham15 cannot be characterised as an eluvial horizon. Besides, an eluvial horizon may have needed much more than three centuries to form.

Similarities are observed between the reddish units (U3 at Cham6 and U5 at Cham15) and the natural soil substrate (U3/U4, Cham6 UpH), interpreted as local sediment. The latter was scraped from around the CP and dumped on the slope to build a working platform for charcoal production (Figure 3). The lack of biological microtraces in this formation and the sharp limit at the contact point between the upper and lower units reveal very little postdepositional biological activity. This is obvious in such a sandy acidic environment where forest soils may only be locally reworked by mammals (surface scratching, burrowing, etc.) or trees (roots, wind-throw, etc.).

The grey units further down (U4 at Cham6, U5a at Cham15), with a better structured porphyritic groundmass, rich in organic fragments and with an increase in total carbon and OM, are assumed to be the top organic horizon of a palaeosol buried under the human-made platform. The band's horizontal orientation and position at the CP's very base and the top of the deeply buried U4 (Cham6) and U5a (Cham15) horizons are related to a post-platform construction pedogenesis discussed below.

The last sandy reddish-orange bottom units U5 (Cham6) and U6 (Cham15) are interpreted as mineral horizons of the ancient profiles buried under the CPs. The high pH_{water} values measured at Cham6 likely result from the washing of vertical ash dissolution products (like Ca^{2+}).

All the dark units, from both CPs Cham6 and Cham15, correspond to charcoal hearth residue accumulations and are regrouped in sequence S3. The next sequence S2 includes sediments disturbed by the platform construction. The last sequence S1 corresponds to the natural undisturbed profile buried under the platforms.

Following Baize and Girard (2009), all the units can be renamed according to the RP. All the black charcoal residue accumulations from both CP Cham6 and Cham15 correspond to the charcoal hearth and can be considered from an archaeological point of view (ar) and called Z_{ar}. The dumped units (U3 from Cham6 and U5 from Cham15) are horizons of human origin (Z) including local geological material (tr) scraped from upslope to construct the platform and are called Ztr. At Cham6, the nondisturbed lower U4 is a buried organomineral horizon unit called $_{II}$A. As it was locally slightly disturbed in clumps during the platform construction process, the U5a from Cham15 unit may be linked to the S2 sequence and called ($_{II}$A) Ztr. The bottom units U5 (for Cham6) and U6 (for Cham15) are similar to the minerogenic slope substrate deposit and are defined as a probable $_{II}$BP horizon.

As the complex soil sequences (Cham6/Cham15) related to the charcoal mound and platform construction result from anthropogenic processes, it is difficult to class the CP soil sequences in the different soil systems. Using the international soil reference group (WRB, 2015), and following the denomination used by Hirsch et al. (2017), the CP soil sequences are attributed to *technosols*, as the dark horizons are linked to industrial production. Also, these dark horizons cannot be called *pretic* as commonly mentioned in the dark-earth archaeological contexts as, in our study, they cannot be linked to agricultural practices. Based on the same arguments, the soil sequence can be more precisely defined as an *anthroposol archéologique artificiel* in the French repository (RP; Baize & Girard, 2009).

4.2 | Charcoal production processes and their impact on soils

4.2.1 | Platform preparation

To stack the wooden logs on the slopes, charcoal makers constructed horizontal flat platforms, burying the natural soil. Compared to other pedological contexts, this homogeneous sandy material does not have a benchmark level (e.g., the Bt horizon in luvic cambisol) that can remain recognisable even after anthropogenic disturbances (Gebhardt, 2021). At the top of the Cham6 buried sequence (U4, Figure 3), the $_{II}$A horizon appears surprisingly thick (20 cm) compared to the natural organomineral horizon of forest soil (i.e., the 10 cm of the A_e horizon from the current entic podzol UpH). To explain this thickness, several nonexclusive hypotheses can be advocated. The first two assumptions are related to charcoal construction, and the third is related to a pedogenetic process.

In the first hypothesis, the U4 unit would have included the organomineral horizon (A) topped by the organic (O) ones. In their experimental burying of a podzol under an artificial bank at Wareham (Hampshire, GB), Macphail and Goldberg (2017) observed compaction of the humus and the organomineral horizons. They showed that lignin (bark, charcoal, etc.) is less sensitive to degradation and can still be observed after 30 years of burial. Unfortunately, the very top of the undisturbed U4 unit (Cham6) was not sampled, and it was impossible to check the possible disorganisation of the structure. Nonetheless, in the sampled upper half of the grey unit, the nonbirefringent decayed pale-coloured vegetal residues observed in the thin section can be related to residual resistant organic elements of lignin. However, in the dry and well-drained acidic environment of Cham6, the longer burial duration (more than 200 years) implies that noncarbonised lignin would decay faster than for the Wareham experiment.

According to the second hypothesis, the upper part of the U4 unit might have been slightly reworked and corresponds to a first terracing level made of the ancient A horizon scraped UpH first. On top of this level, horizons B and Dsi were dumped in an inverted profile to construct the platform (U3). The same process would explain the local reworking of the buried $_{II}$A horizon at Cham15. In the upper part of U4 from Cham6, the observation of articulated phytoliths compressed between sand grains may reinforce this hypothesis. These in situ residual grass leaves, featuring compaction around quartz sand grains observed about 10 cm below the top of the grey level (U4), point to the position of the former natural soil surface. The phytoliths of these grasses are still connected, indicating a lack of disturbance after their burial. The upper part of the observed grey unit (U4) could thus correspond to the dumping of organic and organomineral horizons on the former

natural surface and could explain the thickness of this $_{II}$A horizon. In the upper grey unit (U4), strong horizon mixing is attested by the poor preservation, the disarticulated occurrence, and the distribution (isolated and clustered) of the few RONDEL and ELONGATE ENTIRE phytoliths and by the broken aspect of the latter (Vrydaghs et al., 2016, 2017).

The local UpH current soil (Cham6) is an *entic podzol*, with a poorly expressed eluvial horizon A_e and a low pellety polymorphic structured BP rich in Al and Fe. The last hypothesis is based on the assumption that former harsh climatic conditions and/or anthropogenic land use change could have exacerbated podzolisation processes through low OM mineralisation (Baize & Girard, 2009; Duchaufour, 1983), favouring OM accumulation over a thickness of more than 30 cm. Indeed, on this north-western facing slope, the CP would have been used by the end of the cold and wet medieval Little Ice Age (mid-14th/mid-19th centuries). Podzolisation can be a relatively rapid process. In Greenland, on well-drained granitic moraines, Alexander and Burt (1996) advocate 70 years for the development of an albic (E) horizon and a proto-BP horizon formation, while a well-developed podzolic horizon appears after about 240 years. Also, in the present-day deciduous vosgian forest, Guillet (1987) notes several-centuries-old *entic podzol* development with a high iron content, aluminium/iron translocation, precipitation and alteration processes succeeding one another in soils very dependent on vegetation or climatic conditions (Holm Jakobsen, 1989). So, past anthropogenic activities may also have an indirect influence on podzolisation. Also, Macphail and Goldberg (2017) give examples of early human-induced podzolisation processes with the development of a BP polymorphic pellety structure in only 300 years of Neolithic clearance. This process may have been induced by humans consecutively to biomass exportation, linked to nearly 300 years of charcoal-making activities in this area, as evidenced by charcoal dating, demand for fuel for forges and the degraded state of the local forest in the mid-18th century. Tree cutting, a high coppicing rate, wood species selection and the regular extraction of OM to clean the areas and avoid fires may also have influenced rapid acidification and accelerated podzolisation processes. Due to a lack of sampled sediment material, we unfortunately have no information on the Al_{ox} and Fe_{ox} concentrations in this lower unit U5 (Table 4).

4.2.2 | Charcoal manufacturing process

Along with the charcoal production process, marked topsoil removal during platform preparation accounts for the difficulty described by Gocel-Chalté et al. (2020) when trying to identify evidence of soil horizon formation during regular long breaks in the use of the CPs. Also at Cham6, *Betula* and *Prunus* (Figure 9), not commonly used for charcoal production, might have supplied small branches used to fill the gaps between the logs of the wood pile to avoid large-sized oxygen pockets.

The lack of layering often observed in the thick homogenised black layer at the top of the CPs (i.e., Cham6; Figure 2b) does not indicate that there were no breaks in the use of the CP, but rather the remains from its last use. On the other hand, the greyish aspect of units U3/U4 (Cham15) is not due to a pedogenetic colour fading of the charcoal residual layer (see Section 4.1.2) and may result from anthropogenic factors. This greyish charcoal-depleted layer can thus be assimilated to *frasil* remains from the previous carbonisation. The latter, considered noninflammable, could have been spread to level a previously decayed CP surface.

In both Cham6 and Cham15 residual combustion layers (S3), charcoal identification reveals the use of local taxa, such as *Quercus*, *Fagus*, *Prunus*, *Betula* and undetermined broad-leaved trees (angiosperms) in different proportions. The absence of *Fagus* charcoal in the whole Cham15 profile and its presence in Cham6 also means that the charcoal burners used different local resources from one charcoal place to another.

The lack of *Fagus* charcoal in the palaeosol and the platform at Cham15, unlike Cham6, could point to the fact that the platforms were made with the mineral sediment surrounding each charcoal production place.

4.2.3 | Illuvial iron-organic clay bands developed in the CP

Podzolisation is linked to mineral destruction, even in pedogenetic clays, through acidic organic compounds produced by thick humus. Late glacial colluvium derived from sandstones still contains 5%–8% clay (Guillet et al., 1979) which fits with the data in Table 3.

This low clay content was leached downwards through mechanical transfers and later mixed with the amorphous polymorphic pellets from the podzolic horizons in formation (Guillet et al., 1975; Rouiller et al., 1984). The clayey/iron/organic horizontal bands (lamellae) observed in the CP and the underlying buried A horizon are colloidal migration features often observed in sandy to sandy–loamy acidic archaeological contexts (Féliu & Gebhardt, 2010; Lisa et al., 2019; Thomas et al., 2020). This process, called bathyluvic leaching, precedes the development of the podzolic horizon (Baize & Girard, 2009). It can be favoured by a slight pH variation of short duration which results from anthropogenic activities, such as carbonate inputs in acidic soils (Ampe & Langohr, 2003; Crombé et al., 2015; Langohr, 2001), or soil acidification practices, such as forest grazing, litter extraction or burning (Duchaufour, 1983). In our case, ash production during charcoal burning could have been the main factor causing an increase in pH, even if litter extracted for CP preparation could also have influenced the process. So, for almost three centuries, successive iron and clay band migration could be associated with phases of CP operating. Also, the absence of dust particles (phytolith, charcoal, etc.) and silts in these bands implies a lack of silty material translocation from the surface towards the CP profile. This also suggests that one or a set of iron/clay bands could be linked to a period of CP operating.

For future works in the same acidic context, it would thus be interesting to explore to what extent each lamellae level could correspond to a single charcoal production phase.

4.2.4 | Impact of charcoal combustion on soils

As the local colluvial ferruginous sandstone was originally very porous, poor in matrix and already reddish coloured, the change in colour between the CP profile and the present-day soil is not easy to identify due to the low expected temperatures in the charcoal production process. Apart from under the central chimney, charcoal hearth temperature does not reach more than 400°C (Dupin et al., 2019). Following the literature, soil 'caramelisation' occurs at 100/150°C, and charring starts at 200°C (Mallol, Hernández, Cabanes, Machado, et al., 2013). Phytolith opal starts melting at around 500°C (Boardman & Jones, 1990; Yost, 2008). So, in our case, the burning effect could only be visible in the form of loose, noncrystallised opaque particles and fluorescent and melted phytoliths.

Charcoal or wood char involves the in situ transformation of solid organic wood by combustion below 700°C, keeping the morphology of the original woody precursor. Organic spheroidal tar fragments differ from woody fragments on account of their vesicles, cracks and drop-like anatomy (Lambrecht et al., 2021). Tar/soot is mostly composed of carbon-volatile molecules released by pyrolysis, enriched in PAH and recombined by condensation/precipitation. In the Brandeburger acidic sandy soils, Hirsch et al. (2018) attribute the origin of blackish microscopic aggregates and grain coatings, observed in and under the relict charcoal hearth remains, to tar accumulation from pine combustion. It is difficult to differentiate them under the optical microscope, but strongly charred vegetal, soot/tar and charcoal can be distinguished by their structural organisation (Huisman et al., 2019; Lambrecht et al., 2021; Mallol, Hernández, Cabanes, Sistiaga, et al., 2013). In our case, the charcoal remains did not reveal any microscopically detectable presence of tar/soot indices. The observed blackish aggregates would rather be related to mesofaunal activity, and the dark-reddish-black coatings surrounding the sand grains, even in the UpH profile, should be attributed to the relict of ferruginous cement consolidating the sandstone. Unlike the Brandeburger example, where charcoal burners used much pine-producing tar (Hirsch et al., 2018), Gocel-Chalté et al. (2020) found very few pine macrocharcoal residues on Cham6 and Cham15 CPs, which could explain the lack of tar aggregates observed in our thin sections.

PAC distributions are commonly observed in soils impacted by forest fires (Vergnoux et al., 2011). Fagernas et al. (2012) found distributions of PACs extracted from fresh charcoal and from tars also dominated by naphthalene, fluorene, phenanthrene, and dibenzofuran. Thus, PAC distributions in U1 and U2 (CP Cham6) can be attributed to the abundance of charcoal and tars in these units. Their absence in the platform layer U3 and their very different distribution in UpH soils suggest that these PACs are associated with a solid matrix (charcoal, tar balls) that does not migrate deeper than the level of residual charcoal accumulation.

Combustion of wood produces high-molecular-weight PAHs sorbed to charcoal on the CP and to soot that may also be found in surrounding present-day UpH soil profiles. Due to their very low specific surface, quartz grains should not have sorbed PAHs. At Cham6, the PAH analytic signature decreases downwards in the UpH profile and becomes insignificant in U3 (Figure 5). PAHs are present in the relict charcoal layers but are almost absent in the CP. As PAHs are mostly sorbed to the charcoal produced in the charcoal hearth, this shows that most of them do not migrate downwards and confirms the lack of vertical bioturbation observed in the field and under the microscope. This also confirms the fact that the small charcoal observed in the U3 unit does not belong to the batch produced in the charcoal hearth. In this forested area, despite specific localised erosion (tracks, wind-thrown trees, intentional destruction, etc.), the lateral dispersion of PAHs may also be low. Also, charcoal burners scraped the surrounding soil horizons to construct the flat CP.

4.3 | Past environmental evolution revealed by CP profile analysis

The microscopic mineral grains and very small rounded charcoals wrapped in a silty and slightly birefringent quite thick coating (Figure 4h) were observed in the UpH reference profile (U3), in the CP sediment (U3) and also in the soil buried underneath the CP (U4), formed before CP construction. They cannot be attributed to the previously described podzolic pedogenetic process as they are thicker, silty and slightly birefringent. Some authors attribute these silty coatings to slash-and-burn cultivation, where charcoals and mineral grains are reworked and rolled in the soil by cultivation implements (Ponomarenko et al., 2018) or up-thrown trees (Macphail & Goldberg, 2017). But as ploughing traces (Deák et al., 2017; Gebhardt, 1999; Macphail et al., 1990) have not been observed in the ancient buried soil, nor articulated phytoliths derived from cultivated cereals, an agrarian process cannot be considered here. Moreover, ancient cultivation is unlikely on such steep slopes. Therefore, these relict features might be natural phenomena due to quaternary cryogenic and melting processes (Van Vliet-Lanoë et al., 2004), slope creeping (Bertran, 2004) or wind shake (Macphail & Goldberg, 2017) on naked surfaces throughout or before the Holocene.

As seen above, the palaeosols were more (Cham15) or less (Cham6) superficially disturbed but well-preserved due to rapid burial under 70 cm of dumped platform sediments and charcoal mound residues. They may be representative of past ecological conditions. This would account for some of the differences observed between the ancient soil sequence (S1) and the present-day UpH one.

In the UpH acidic soil context, the lack of vertical mixing in the A_e horizon points to the integrity of the phytolith records.

This view is further supported by the non-translocation of fine particles in these soils and the absence of phytoliths and charcoal dust in the bands observed in the deep horizons of the Cham6 CP. These traits, together with the observation of phytoliths in plant fragments and tissues (*senso* Stoops, 2003), tend to support the view that the phytolith assemblage recovered by extraction reflects present-day plant cover, namely a mixed deciduous woodland (Figure 7b). Nevertheless, an over-representation of grass phytoliths linked to the disaggregation of sand grain clay coatings is more likely.

Consequently, phytoliths (including some burnt and melted ones) associated with very small undefined microcharcoals integrated into the coatings recorded in the UpH slope deposit (UpHPhU3; Figure 3) can be considered as background noise resulting from interglacial or later Holocene colluviation.

Phytolith analysis shows a more marked presence of grass-derived phytoliths in the buried organic soil horizon (CPPhU4; Figure 7b). We cannot rule out the possibility that the latter record is also partly biased, this time by the specific grass phytolith features observed in the thin section, but the presence of grasses was nonetheless definitely more marked in the past. Past vegetation cover would have been more open than the present-day record. Historical sources are of some relevance here, as they document ancient glasswork, which was highly prejudicial to the forest (Jehin, 2010). Glass makers intensively collected ferns and small branches for ash and potash supply, along with medium-sized dry beech/oak wood for glass fusion (Jehin, 2005). This must have contributed to local forest degradation to a much greater extent than cattle grazing and uncontrolled wood gathering by peasants for their own needs. This would have favoured *graminae* development before the onset of charcoal-making activities in the Cham6 area. Wood exploitation was regulated by law in 1771 to prevent disorganised wood gathering (Rochel, 2017). Then, grass growing was probably stimulated during the regular forest opening required for supplying wood for charcoal making.

In the palaeosol upper horizon (U4, Cham6), melted and autofluorescent phytoliths point to the burning of diverse plant materials (Devos et al., 2021), possibly also related to glass-makers and coaler settlements (Burri, 2008). Cultivation involving slash-and-burn practices (Macphail & Goldberg, 2017) was unlikely on such steep acidic slopes.

The similarity of the charcoal taxa identified in S2 and S1 for both CPs (Figure 9c,d) also reflects local vegetation trends. Furthermore, the lack of carbonised *Fagus* fragments in the buried soil of Cham15 indicates forest heterogeneity and demonstrates that charcoal burners used pre-existing resources found around each CP. The 'small' ligneous tree charcoal from light-demanding species (*Betula* and *Prunus*; Figure 9c) results from more or less forest disturbances. The observation of only undefined angiosperms in the S1 palaeosol (Cham15) might be related to more intensive disturbance than in Cham6.

Finally, charcoal and phytolith identification in the palaeosol revealed a degraded environment which may corroborate the poor state of the forest reported in the topographical atlas of the county of Bitche from the mid-18th century (Anonymous, 1758; Robin, 2006; Rochel, 2017). Perhaps this degraded area was chosen for charcoal burning precisely because it was more suitable to start coppice management.

5 | CONCLUSION

This multidisciplinary study of soil profiles associated with well-preserved charcoal-making platforms from the 18th century and located in low mountains near Bitche (northern Vosges, France) helped decipher the impact of ancient charcoal-making activities on soils. Field and analytic soil observations are completed by pedogenetic features, charcoal and phytolith analysis, and molecular analyses of organic pollutant content. In addition to enhancing our knowledge of the construction and use(s) of CPs, this sequence documents local past environmental evolution, soil evolution and postabandonment processes.

The complex CP *technosol* is an ancient natural soil sequence buried by a man-made platform on which charcoal accumulated. The UpH current soil is an *entic Podzol*. The acidic and slightly bioturbated context provides reliable information on past ecological conditions in the buried soil. It transpires that local soil podzolisation started before platform construction. Despite localised strong soil acidity, ash production induced low alkalinisation of the charcoal hearth, some remains of which are still faintly detectable three centuries after abandonment. PAHs identified in the CP soil originate from the tar produced during wood carbonisation. Sorbed on charcoal, they have persisted in soils, preserving their very recognisable distribution through the centuries. This specific PAH contribution is restricted to the CP soil and we have no evidence that charcoal-making activities contributed to the global diffuse pollution, although this hypothesis cannot be excluded.

PH variations related to the cyclic reuse of the CP-induced iron/clayey/organic band formation in the platform sediment and the buried soil. Despite lower taxonomical diversity on thin sections, quantitative and qualitative general trends in the composition of charcoal assemblages still yield relevant taxonomical information. The taxonomical spectra for both hearths are similar, with mainly *Quercus*, *Fagus*, some *Betula* and very occasional *Prunus*. Phytolith assemblages from the palaeosol, together with historical sources, suggest a less dense forest cover before charcoal-burning activities. This degraded canopy, also reported by an ancient forestry archive, may result from mismanagement before wood-coppicing regulations aimed at improving charcoal production.

AUTHOR CONTRIBUTIONS

Anne Gebhardt: Writing—original draft; writing—review and editing; investigation; methodology; conceptualisation; visualisation; supervision. **Anne Poszwa**: Funding acquisition; writing—original

draft; writing—review and editing; methodology; investigation; project administration; conceptualisation; visualisation; supervision. **Laurence Mansuy-Huault**: Funding acquisition; methodology; investigation; writing—original draft; visualisation; conceptualisation; writing—review and editing. **Vincent Robin**: Visualisation; conceptualisation; writing—original draft; writing—review and editing; methodology; investigation. **Luc Vrydaghs**: Visualisation; writing—original draft; writing—review and editing; conceptualisation; methodology; investigation. **Catherine Lorgeoux**: Methodology; writing—original draft.

ACKNOWLEDGEMENTS

The authors would like to thank the 'Observatoire Homme/Milieu de Bitche' project (OHM Bitche, France), which offered the opportunity to participate in the interdisciplinary studies conducted there. This research was financed by the Interdisciplinary Research Device on Human-Environment Interactions called 'Labex Driihm' (CNRS) and the Earth and Environment Observatory of Lorraine (OTELo, Lorraine University, Nancy, France). Thanks to Rosalie Hermans (MARI–VUB) for having processed the phytoliths bulk samples at the Royal Belgian Institute of Natural Sciences. Special thanks to Xavier Rochel (Lorraine University, LOTERR) for providing us with the topographical atlas of the county of Bitche (A.D.M. B 10139, B 10140), which allowed us to compare the palaeoenvironmental results with the historical forest description established in 1758. The authors also warmly thank Richard I. Macphail (Institute of Archaeology, University College London) and Paul Goldberg (Institut für Naturwissenschaftliche Archäologie, University of Tübingen) for their review and constructive comments on this manuscript. The authors will not forget Neil Hucker, Margaret Shanahan and Louise Byrne for their help in improving the text in English. Final thanks to the two anonymous reviewers who agreed to proofread this paper.

CONFLICT OF INTEREST STATEMENT

The authors declare no conflicts of interest.

DATA AVAILABILITY STATEMENT

The data that support the findings of this study are available from the corresponding author upon reasonable request.

ORCID

Anne Gebhardt https://orcid.org/0000-0003-1847-4338

REFERENCES

Abuhelou, F., Mansuy-Huault, L., Lorgeoux, C., Catteloin, D., Collin, V., Bauer, A., Kanbar, H. J., Gley, R., Manceau, L., Thomas, F., & Montargès-Pelletier, E. (2017). Suspended particulate matter collection methods influence the quantification of polycyclic aromatic compounds in the river system. *Environmental Science and Pollution Research*, *24*(28), 22717–22729. https://doi.org/10.1007/s11356-017-9840-5

Alexander, E. B., & Burt, R. (1996). Soil development on moraines of Mendenhall Glacier, southeast Alaska. 1. The moraines and soil morphology. *Geoderma*, *72*(1–2), 1–17. https://doi.org/10.1016/0016-7061(96)00021-3

Allaby, M. (2008). *Dictionnary of Earth sciences*. Oxford University Press.

Ampe, C., & Langohr, R. (2003). *Project waardevolle bodems in Vlanderen* (Report, LaBod/stud 2004, 0102). http://researchgate.net/publication/315613503

Anonymous. (1758). *Mémoires Concernant l'arpentage de la Forest de Bitche Pour servir Au Rétablissement et l'amélioration de cette Forêt Divises Suivant l'ordre des Forêteries et des Bans dans lesquels On trouvera la quantité superficielle de chaque Canton, de Prés, Terres et Bois, la qualité du sol, l'espèce de bois qu'il contient, son Etat de deperissement, avec la quantité qu'on doit mettre en vente, tant en Bois de hollande qu'en Bois de corde, avec quelques autres mémoires particuliers également propres à faciliter le Rétablissement de cette Forêt contenant : Foresteries, ou la partie couverte. Première Partie. Mémoires sur les 7 Foresteries du Comté de Bitche*, plan III, p.24 (source A.D.M. B 10139, B 10140).

Babel, U. (1975). Micromorphology of soil organic matter. In E. J. Gieseking (Ed.), *Soil components* (pp. 369–473). Springer.

Baize, D. (2000). Guide des analyses en pédologie, *coll*. Techniques et pratiques INRA.

Baize, D., & Girard, M. C. (2009). *Référentiel pédologique*. Association Française pour l'Étude du Sol.

Baize, D., & Jabiol, B. (1995). *Guide pour le description des sols*. INRA.

Beckmann, T. (1997). Präparation bodenkundlicher Dünnschliffe für mikromorphologishe Untersuchungen. In K. Stahr (Ed.), *Mikromorphologische Methoden in des Bodenkunden* (Vol. 40, pp. 89–103). Hohenheimer Bodenkundlicher Hefte.

Bell, M. J., & Worrall, F. (2011). Charcoal addition to soils in NE England: A carbon sink with environmental co-benefits? *Science of the Total Environment*, *409*(9), 1704–1714. https://doi.org/10.1016/j.scitotenv.2011.01.031

Bertran, P. (2004). *Reptation. Dépôts de pente continentaux, dynamique et faciès*, P. Bertran (dir.), *Quaternaire*, Hors Série no. 1 (pp. 80–83).

Biache, C., Lorgeoux, C., Colombano, S., Saada, A., & Faure, P. (2021). Multistep thermodesorption coupled with molecular analyses as a quick, easy and environmentally friendly way to measure PAH availability in contaminated soils. *Talanta*, *228*, 122235. https://doi.org/10.1016/j.talanta.2021.122235

Boardman, S., & Jones, G. (1990). Experiments on the effects of charring on cereal plant components. *Journal of Archaeological Science*, *17*, 1–11. https://doi.org/10.1016/0305-4403(90)90012

Bonhage, A., Hirsch, F., Schneider, A., Raab, A., Raab, T., & Donovan, S. (2020). Long term anthropogenic enrichment of soil organic matter stocks in forest soils—Detecting a legacy of historical charcoal production. *Forest Ecology and Management*, *459*, 117814. https://doi.org/10.1016/j.foreco.2019.117814

Borchard, N., Ladd, B., Eschemann, S., Hegenberg, D., Möseler, B. M., & Amelung, W. (2014). Black carbon and soil properties at historical charcoal production sites in Germany. *Geoderma*, *232/234*, 236–242. https://doi.org/10.1016/j.geoderma.2014.05.007

Bortolini, M., Agnoletto, F. C., Argiriadis, E., Nicosia, C., McWethy, D. B., Devos, Y., Stortini, A. M., Baldan, M., Roman, M., Vendrame, T., Scaggiante, R., Bruno, B., Pojana, G., & Battistel, D. (2022). Insight into the carbonaceous fraction of three cultural layers of different age from the area of Verona (NE Italy). *Catena*, *217*, 106453. https://doi.org/10.1016/j.catena.2022.106453

Bourne, D., Fatima, T., van Meurs, P., & Muntean, A. (2014). Is adding charcoal to soil a good method for CO_2 sequestration?—Modeling a spatially homogeneous soil. *Applied Mathematical Modelling*, *38*(9), 2463–2475. https://doi.org/10.1016/j.apm.2013.10.064

Bucheli, T. D., Blum, F., Desaules, A., & Gustafsson, Ö. (2004). Polycyclic aromatic hydrocarbons, black carbon, and molecular markers in soils

of Switzerland. *Chemosphere*, *56*, 1061–1076. https://doi.org/10.1016/j.chemosphere.2004.06.002

Bullock, P., Fedoroff, N., Jongerius, A., Stoops, G., Tursina, T., & Babel, U. (1985). *Handbook for soil thin section description*. Waine Research Publication.

Burri, S. (2008, June 6). *Enquête ethnoarchéologique sur le mode de vie et lesavoir-faire des derniers charbonniers de Calabre (Italie) : Entre tradition etmodernité. Cultures, economies, sociétés et environnement du début de la préhistoire au Moyen-Age : Travaux en cours*, A. Boutet, C. Defrasne, T. Lachenal (dir.), Actes de la troisième table ronde des jeunes chercheurs enarchéologie de la MMSH, Aix-en-Provence. http://researchgate.net/publication/275210766

Calvet, J.-P. (2012). *Les charbonniers de la Montagne Noire*. Les Cahiers de la Société d'Histoire de Revel Saint-Ferréol. http://www.lauragais-patrimoine.fr/PATRIMOINE/CHARBONNIERES/CHARBONNIERES.html

Conedera, M., Tinner, W., Neff, C., Meurer, M., Dickens, A. F., & Krebs, P. (2009). Reconstructing past fire regimes: Methods, applications, and relevance to fire management and conservation. *Quaternary Science Reviews*, *28*, 555–576. https://doi.org/10.1016/j.quascirev.2008.11.005

De Conninck, F., & Righi, D. (1981). Podzolization and the spodic horizon. In P. Bullock & M. P. Murphy (Eds.), *Soil micromorphology, soil genesis* (Vol. 2, pp. 389–418). A.B.A. Publishers.

Crombé, P., Langohr, R., & Louwagie, G. (2015). Mesolithic hearth-pits: Fact or fantasy? A reassessment based on the evidence from the sites of Doel and Verrebroek (Belgium). *Journal of Archaeological Science*, *61*, 158–171. https://doi.org/10.1016/J.JAS.2015.06.001

Deák, J., Gebhardt, A., Lewis, H., Usai, M. R., & Lee, H. (2017). Soils disturbed by vegetation clearance and tillage. In C. Nicosia & G. Stoops (Eds.), *Archaeological soil and sediment micromorphology* (pp. 231–264). Wiley & Sons Ltd. https://doi.org/10.1002/9781118941065.ch28

Deforce, K., Vanmontfort, B., & Vandekerkhove, K. (2018). Early and high medieval (c. 650 AD–1250 AD) charcoal production and its impact on woodland composition in the Northwest-European lowland: A study of charcoal pit kilns from sterrebeek (Central Belgium). *Environmental Archaeology*, *26*(2), 168–178. https://doi.org/10.1080/14614103.2018.1538087

Devos, Y., Hodson, M., & Vrydaghs, L. (2021). Autofluorescent phytoliths: A new method for detecting heating and fire. *Environmental Archaeology*, *26*(4), 388–405. https://doi.org/10.1080/14614103.2020.1777056

Duchaufour, P. (1955). Les sols des forêts résineuses des Basses-Vosges. *Revue Forestière Française*, *7*(9–10), 675–687. https://doi.org/10.4267/2042/27131

Duchaufour, P. (1983). *Pédogenèse et classification, pédologie* (Vol. 1). Masson.

Duhamel du Monceau, H. L. (1761). *Artdu charbonnier, ou manière de faire le charbon. Description des arts etmétiers, faite ou approuvée par MM de l'Académie des Sciences*. Desaint et Saillant.

Dupin, A., Girardclos, O., Fruchart, C., Laplaige, C., Nuninger, L., Dufraisse, A., & Gauthier, E. (2017). Anthracology of charcoal kilns in the forest of Chailluz (France) as a tool to understand Franche-Comte forestry from the mid-15th to the early 20th century AD. *Quaternary International*, *458*, 200–213. https://doi.org/10.1016/j.quaint.2017.03.008

Dupin, A., Sordoillet, D., Fréville, K., Girardclos, O., & Gauthier, E. (2019). The taphonomic characterization of a charcoal production platform. contribution of an innovative pair of methods: Raman analysis and micromorphology. *Journal of Archaeological Science*, *107*, 87–99. https://doi.org/10.1016/j.jas.2019.05.003

Fagernas, L., Kuoppala, E., & Simell, P. (2012). Polycyclic aromatic hydrocarbons in birch wood slow pyrolysis products. *Energy & Fuels*, *26*(11), 6960–6970. https://doi.org/10.1021/ef3010515

Féliu, C., & Gebhardt, A. (2010). *La fortification de la Heidenstadt à Ernolsheim-lès-Saverne (Bas-Rhin)*, Rapport de recherche, UMR 7044. https://shs.hal.science/halshs-01143668

Food and Agriculture Organization of the United Nations. (1987). Simple technologies for charcoal making (FAO Forestry Paper, 41). http://fao.org/3/X5328e/x5328e00.htm#Contents

Fouédjeu, L., Saulnier, M., Lejay, M., Dušátko, M., Labbas, V., Jump, A. S., Burri, S., Buscaino, S., & Py-Saragaglia, V. (2021). High resolution reconstruction of modern charcoal production kilns: An integrated approach combining dendrochronology, micromorphology and anthracology in the French Pyrenees. *Quaternary International*, *593/594*, 306–319. https://doi.org/10.1016/j.quaint.2020.11.033

Garnier, E. (2004). *Terre de conquête. La forêt vosgienne sous l'ancien régime*. Fayard.

Gebhardt, A. (1991). *Evolution du paléopaysage agricole dans le nord-ouest de la France : Apport de la micromorphologie* [Thèse, de l'Université de Rennes]. https://hal.archives-ouvertes.fr/tel-02176386

Gebhardt, A. (1999). Micromorphological analysis of soil structural modification caused by different cultivation implements. Prehistory of agriculture, new experimental and ethnographic approaches. In P. Anderson (Ed.), *Monographie du CRA* (Vol. 40, pp. 260–266). Institute of Archaeology, University of California.

Gebhardt, A. (2007). Impact of charcoal production activities on soil profiles: The micromorphological point of view. *ArchéoSciences*, *31*, 127–136. https://journals.openedition.org/archeosciences/833

Gebhardt, A. (2008). *Impact anthropique anciens sur les sols forestiers. Quelques études de cas en contexte archéologique et expérimental*. La mémoire des forêts, Forêt, archéologie et environnement Colloque Sylva, Déc 2004, INRA Nancy (pp. 211–218). http://hal-02064272

Gebhardt, A. (2021). *Montiers-sur-Saulx, Rapport d'analyse micromorphologique desols de placettes de charbonnage*. Programme Deepsurf Université deLorraine, CNRS, LIEC UMR 7360 F-5000, Vandœuvre-lès-Nancy. http://hal-03513258

Gebhardt, A., Occhietti, S., & Fechner, K. (2014). Grandes phases de pédogenèse, d'érosion et d'anthropisation des sols au cours de la seconde moitié de l'Holocène en Lorraine (France). *ArchéoSciences*, *38*, 7–29. https://doi.org/10.4000/archeosciences.4113

Gocel-Chalté, D., Guerold, F., Knapp, H., & Robin, V. (2020). Anthracological analyses of charcoal production sites at a high spatial resolution: The role of topography in the historical distribution of tree taxa in the Northern Vosges mountains, France. *Vegetation History and Archaeobotany*, *29*, 641–655. https://doi.org/10.1007/s00334-020-00769-z

Goldberg, P., Lev-Yadun, S., & Bar-Yosef, O. (1994). Petrographic thin sections of archaeologial sediments: A new method for paleobotanical studies. *Geoarchaeology*, *9*(3), 243–257. https://doi.org/10.1002/gea.3340090305

Groenman-van Waatering, M., & Robinson, M. (1988). *Man-made soils*. BAR International.

Guillet, B. (1987). L'âge des Podzols. In Righi et Chauvel (Ed.), *Podzol et podzolisation* (pp. 131–146). AFES.

Guillet, B., Rouiller, J., & Souchier, B. (1975). Podzolization and clay migration in spodosols of eastern France. *Geoderma*, *14*(3), 223–245. https://doi.org/10.1016/0016-7061(75)90003-8

Guillet, B., Vedy, J.-C., Rouiller, J., & Souchier, B. (1979). Migrations de particules argileuses dans les milieux de géochimie organique très acide : Exemple des podzols sur colluvium de grès vosgien. *Sciences Géologiques, Bulletins et Mémoires*, *53*(1), 13–18.

Hardy, B., & Dufey, J. E. (2012). Estimation des besoins en charbon de bois et en superficie forestière pour la sidérurgie wallonne préindustrielle (1750-1830). Première partie : Les besoins en charbon de bois. *Revue Forestière Française*, *64*(6), 477–488. https://doi.org/10.4267/2042/48747

Hardy, B., Leifeld, J., Knicker, H., Dufey, J. E., Deforce, K., & Cornélis, J.-T. (2017). Long term change in chemical properties of pre-industrial

charcoal particles aged in forest and agricultural temperate soil. *Organic Geochemistry*, *107*, 33–45. https://doi.org/10.1016/j.orggeochem.2017.02.008

Hirsch, F., Raab, T., Ouimet, W., Dethier, D., Schneider, A., & Raab, A. (2017). Soils on historic charcoal hearths: Terminology and chemical properties. *Soil Science Society of America Journal*, *81*, 1427–1435. https://doi.org/10.2136/sssaj2017.02.0067

Hirsch, F., Schneider, A., Bauriegel, A., Raab, A., & Raab, T. (2018). Formation, classification, and properties of soils at two relict charcoal hearth sites in Brandenburg, Germany. *Frontiers in Environmental Science*, *6*, 6. https://doi.org/10.3389/fenvs.2018.00094

Holm Jakobsen, B. (1989). Evidence for translocations into the B horizon of a subarctic Podzol in Greenland. *Geoderma*, *45*(1), 3–17. https://doi.org/10.1016/0016-7061(89)90053-0

Huisman, D. J., Niekus, M. J. L. T., Peeters, J. H. M., Geerts, R. C. A., & Müller, A. (2019). Deciphering the complexity of a 'simple' mesolithic phenomenon: Indicators for construction, use and taphonomy of pit hearths in Kampen (the Netherlands). *Journal of Archaeological Science*, *109*, 104987. https://doi.org/10.1016/j.jas.2019.104987

INRAe. 2022, *Catalogue analytique général, Laboratoire d'Analyses des sols INRAE, Arras, France*. www6.hautsdefrance.inrae.fr/las

Jabiol, B., Brêthes, A., Brun, J.-J., Ponge, J.-F., Toutain, F., Zanella, A., Aubert, M., & Bureau, F. (2009). Typologiedes formes d'humus forestières sous climats tempérés. *Référentiel pédologique*, D. Baize & M.C. Girard (dir.), Association Française pour l'Étude du Sol. Quae (ed.) (pp. 327-355).

Jamagne, M. (2011). *Grands paysages pédologiques de France*. Synthèses INRA, Quae (ed), Versailles.

Jehin, P. (2005). *Les forêts des Vosges du nord du Moyen-Age à la Révolution Milieux, usages, exploitations*. Presses Universitaires de Strasbourg.

Jehin, P. (2010). *Verriers et forêts sous l'ancien régime en Alsace, Les actes du CRESAT*. https://hal.archives-ouvertes.fr/hal-00559372

Kemp, R. A. (1985). *Soil micromorphology and the quaternary. Technical guide*. Quaternary Research Association.

Kerré, B., Willaert, B., Cornelis, Y., & Smolders, E. (2017). Long-term presence of charcoal increases maize yield in Belgium due to increased soil water availability. *European Journal of Agronomy*, *91*, 10–15. https://doi.org/10.1016/j.eja.2017.09.003

Lambrecht, G., Rodríguez de Vera, C., Jambrina-Enríquez, M., Crevecoeur, I., Gonzalez-Urquijo, J., Lazuen, T., Monnier, G., Pajović, G., Tostevin, G., & Mallol, C. (2021). Characterisation of charred organic matter in micromorphological thin sections by means of Raman spectroscopy. *Archaeological and Anthropological Sciences*, *13*(1), 13. https://doi.org/10.1007/s12520-020-01263-3

Langohr, R. (2001). L'anthropisation du paysage pédologique agricole de la Belgique depuis le Néolithique ancien—Apports de l'archéopédologie. *Etude et gestion des Sols*, *8*(2), 3–118.

Legros, J.-P. (2007). *Les grands sols du monde*. Presses polytechniques et Universitaires Romandes, coll. sciences de la terre.

Lexa-Chomard, A., & Pautrot, C. (2006). *Géologie et Géographie de la Lorraine*. Éditions Serpenoises.

Lisá, L., Bajer, A., Rejšek, K., Vranova, V., Vejrostová, L., Wisniewski, A., & Krištuf, P. (2019). Review of illuvial bands origin; what might the presence of dark brown bands in sandy infillings of archaeological features or cultural layers mean? *Interdisciplinaria Archaeologica—Natural Sciences in Archaeology*, *X*(1), 19–28. https://doi.org/10.24916/iansa.2019.1.2

Ludemann, T., Brandt, M., Kaiser, L., & Schick, L. (2017). Variation of past wood use across local edaphic gradients reflects tree species ecology—Examples of the fine spatial resolution of kiln site anthracology. *Quaternary International*, *458*, 224–232. https://doi.org/10.1016/j.quaint.2017.03.069

Macphail, R., Courty, M.-A., Hathier, J., & Wattez, J. (1997). *The soil micromorphological evidence of domestic occupation and stabling activities, Arene Candide: A functional and environmental assessment of the Holocene sequence: Excavation Bernabo Brea-Cardini 1940-50*. (pp. 53–88) Memorie dell'Instituto Italiano di Paleontologia Umana, nuova serie 5, Il Calamo, Roma.

Macphail, R. I. (1981). The micromorphology of spodosols in catenary sequences on lowland heathland in surrey, England). In P. Bullock & C. P. Murphy (Eds.), *Soil micromorphology* (Vol. 2, pp. 647–653). A.B.A. Publishers.

Macphail, R. I., Courty, M. A., & Gebhardt, A. (1990). Soil micromorphological evidence of early agriculture in North West Europe. *World Archaeology*, *22*(1), 53–69. https://doi.org/10.1080/00438243.1990.9980129

Macphail, R. I., & Goldberg, P. (2017). *Applied soils and micromorphology in archaeology*. Cambridge University Press.

Maillant, S., Party, J. P., Muller, N., Michel, F., Pesy, P., Brauer, M., Bourot, A., Kung, A., Barneoud, C., Labou, L., Purson, L., Vauthier, Q., Vagner, A., Jouart, A., Sauzet, O., Antoine, J. M., & Brouant, B. (2016). *Descriptionde l'Unité Cartographique de Sol (UCS) numéro 6202, étude 3142*. Référentiel régional pédologique de la Lorraine. http://gouv.fr/depot/fiches/INRA

Mallol, C., Hernández, C. M., Cabanes, D., Machado, J., Sistiaga, A., Pérez, L., & Galván, B. (2013). Human actions performed on simple combustion structures: An experimental approach to the study of Middle Palaeolithic fire. *Quaternary International*, *315*, 3–15. https://doi.org/10.1016/j.quaint.2013.04.009

Mallol, C., Hernández, C. M., Cabanes, D., Sistiaga, A., Machado, J., Rodríguez, Á., Pérez, L., & Galván, B. (2013). The black layer of Middle Palaeolithic combustion structures. Interpretation and archaeostratigraphic implications. *Journal of Archaeological Science*, *40*(5), 2515–2537. https://doi.org/10.1016/j.jas.2012.09.017

Mara dos Santos Barbosa, J., Ré-Poppi, N., & Santiago-Silva, M. (2006). Polycyclic aromatic hydrocarbons from wood pyrolyis in charcoal production furnaces. *Environmental Research*, *101*, 304–311. https://doi.org/10.1016/j.envres.2006.01.005

Mastrolonardo, G., Francioso, O., & Certini, G. (2018). Relic charcoal hearth soils: A neglected carbon reservoir. Case study at Marsiliana forest, Central Italy. *Geoderma*, *315*, 88–95. https://doi.org/10.1016/j.geoderma.2017.11.036

Menillet, F., Coulombeau, C., Geissert, F., Konrad, H. J., & Schwoerer, P. (1989). *Notice explicative de la carte géologique, feuille de Lembach à 1/50 000, BRGM, Orléans*.

Mooney, S. D., & Tinner, W. (2011). The analysis of charcoal in peat and organic sediments. *Mires and Peat*, *7*, 1–18.

Murphy, C. P. (1986). *Thin section preparation of soils and sediments*. A.B. Academic Publishers.

Neumann, K., Strömberg, C. A. E., Ball, T., Albert, R. M., Vrydaghs, L., & Cummings, L. S. (2019). International Code for Phytolith Nomenclature (ICPN) 2.0. *Annals of Botany*, *124*(2), 189–199. https://doi.org/10.1093/aob/mcz064

Nicosia, C., & Stoops, G. (2017). *Archaeological soil and sediment micromorphology*. Wiley.

Nolken, W. (2005). *Holzkohle analytische Untersuchungen zur Waldgeschichte der Vogesen* [These, Universiteit Albert-Ludwig, Germany].

Oliveira, C., Bouquerel, J., Rochel, X., Karimi-Moayed, N., Vandenberghe, D., De Grave, J., Deforce, K., Devin, S., & Robin, V. (2022). Woodland management as major energy supply during the early industrialization: A multiproxy analysis in the northwest european lowlands. *Land*, *11*, 555.

Padiam, D., & McDonald, J. (1987). Forest service saves 1889 charcoal kilns. *Society for Industrial Archeology Newsletter*, *16*(4), 1–12.

Pitts Jarvis, J. (1960). *The wood charcoal industry in the State of Missouri*. The University of Missouri Bulletin, 62,21 (Engineering Experiment Station series, p. 48). http://docslib.org/doc/3226362/the-wood-charcoal-industry-in-the-state-of-missouri

Plachá, D., Raclavská, H., Matýsek, D., & Rümmeli, M. H. (2009). The polycyclic aromatic hydrocarbon concentrations in soils in the Region of Valasske Mezirici, the Czech Republic. *Geochemical Transactions*, *10*, 12. https://doi.org/10.1186/1467-4866-10-12

Ponomarenko, E., Tomson, P., Ershova, E., & Bakumenko, V. (2019). A multi-proxy analysis of sandy soils in historical slash-and-burn sites: A case study from Southern Estonia. *Quaternary International*, *516*, 190–206. https://doi.org/10.1016/j.quaint.2018.10.016

Raab, A., Bonhage, A., Schneider, A., Raab, T., Rösler, H., Heußner, K.-U., & Hirsch, F. (2019). Spatial distribution of relict charcoal hearths in the former royal forest district Tauer (SE Brandenburg, Germany). *Quaternary International*, *511*, 153–165. https://doi.org/10.1016/j.quaint.2017.07.022

Van Ranst, E., Wilson, M. A., & Righi, D. (2018). Spodic materials. In G. Stoops, V. Marcelino, & F. Mees (Eds.), *Interpretation of micromorphological features of soils and regoliths* (pp. 633–662). Elsevier.

De Resende, M. F., Brasil, T. F., Madari, B. E., Pereira Netto, A. D., & Novotny, E. H. (2018). Polycyclic aromatic hydrocarbons in biochar amended soils: Long-term experiments in Brazilian tropical areas. *Chemosphere*, *200*, 641–648. https://doi.org/10.1016/j.chemosphere.2018.02.139

Righi, D., & Lorphelin, L. (1987). Structure des microagrégats des sols podzolisés sur micaschistes d'un versant type de l'Himalaya (Nepal). In N. Fedoroff, L.-M. Bresson, & M.-A. Courty (Eds.), *Soil micromorphology* (pp. 295–302). AFES, Plaisir.

Robin, B. (2006). *Le Pays de Bitche il y a 250 Ans* (p. 120). Société d'Histoire et d'Archéologie.

Robin, V., Bork, H.-R., Nadeau, M.-J., & Nelle, O. (2014). Fire and forest history of central European low mountain forest sites based on soil charcoal analysis: The case of the eastern Harz. *The Holocene*, *24*, 35–47.

Rochel, X. (2017). *Une biogéographie historique. Forêts et industries dans le comté de Bitche au XVIII e siècle*. Histoire & Mesure, EHESS. https://hal.archives-ouvertes.fr/hal-02954365

Rodrigues, A. F., Novotny, E. H., Knicker, H., & de Oliveira, R. R. (2019). Humic acid composition and soil fertility of soils near an ancient charcoal kiln: Are they similar to Terra Preta de Índios soils? *Journal of Soils and Sediments*, *19*, 1374–1381. https://doi.org/10.1007/s11368-018-2162-5

Rouiller, J., Brethes, A., Burtin, G., & Guillet, B. (1984). Fractionnement des argiles par ultracentrifugation en continu : Évolution des illites en milieu podzollque/clay fractionation by continuous flow uitracentrifugation : Evolution of illites in a podzolic soil. *Sciences Géologiques Bulletin*, *37*, 319–331. https://doi.org/10.3406/sgeol.1984.1676

Schlosser, C. (2021). *Le charbonnier, une longue histoire*. Images et Découvertes.

Sell, Y., Berchtold, J.-P., Callot, H., Hoff, M., Gall, J.-C., & Walter, J.-M. (1998). *L'Alsace et les Vosges*. La bibliothèque du naturaliste, Delachaux et Niestlé.

Stoops, G. (2003). *Guidelines for analysis and description of soil and regolith thin sections*. Soil Science Society of America.

Stoops, G., Marcelino, V., & Mees, F. (2018). *Interpretation of micromorphological features of soils and regoliths*. Elsevier.

Théobald, N., Perriaux, J., Langenfeld, F., & Both, J. (1967). *Notice de la carte géologique de Bitche Walschbronn* (Vol. XXXVII-13). BRGM.

Thomas, Y., Chenal, F., Courel, B., Delangle, C., Schneider, N., & Gebhardt, A. (2020). *Eckwersheim, Bas-Rhin, Kleine Breite, COS site 5.2*, Grand Est : rapport de fouille, Metz, Inrap GE.

Tinner, W., & Hu, F. S. (2003). Size parameters, size-class distribution and area-number relationship of microscopic charcoal: Relevance for fire reconstruction. *The Holocene*, *13*, 499–505. https://doi.org/10.1191/0959683603hl615rp

Vergnoux, A., Malleret, L., Asia, L., Doumenq, P., & Theraulaz, F. (2011). Impact of forest fires on PAH level and distribution in soils. *Environmental Research*, *111*, 193–198. https://doi.org/10.1016/j.envres.2010.01.008

Verrecchia, E., & Trombino, L. (2021). *A visual atlas for soil micromorphologists*. Springer Open Access. https://doi.org/10.1007/978-3-030-67806-7

Van Vliet-Lanoë, B. (1998). Frost and soils: Implications for paleosols, paleoclimates and stratigraphy. *Catena*, *34*, 157–183. https://doi.org/10.1016/S0341-8162(98)00087-3

Van Vliet-Lanoë, B., & Fox, C. A. (2018). Frost action. In G. Stoops, V. Marcelino, & F. Mees (Eds.), *Interpretation of micromorphological features of soils and regoliths* (pp. 575–603). Elsevier.

Van Vliet-Lanoë, B., Fox, C. A., & Gubin, S. V. (2004). Micromorphology of cryosols. In J. M. Kimble (Ed.), *Cryosols* (pp. 365–390). Springer. https://doi.org/10.1007/978-3-662-06429-0_18

Vrydaghs, L., Ball, T. B., & Devos, Y. (2016). Beyond redundancy and multiplicity. Integrating phytolith analysis and micromorphology to the study of Brussels Dark Earth. *Journal of Archaeological Science*, *68*, 79–88. https://doi.org/10.1016/j.jas.2015.09.004

Vrydaghs, L., & Devos, Y. (2018). Phytolith analysis of soil and ceramic thin sections. In C. L. Smith (Ed.), *Encyclopedia of global archaeology*. Springer. https://doi.org/10.1007/978-3-319-51726-1_3286-1

Vrydaghs, L., & Devos, Y. (2020). Visibility, preservation and colour: A descriptive system for the study of Opal Phytoliths in (archaeological) soil and sediment thin sections. *Environmental Archaeology*, *25*(2), 170–177. https://doi.org/10.1080/14614103.2018.1501867

Vrydaghs, L., Devos, Y., & Petô, A. (2017). Opal phytoliths. In C. Nicosia & G. Stoops (Eds.), *Archaeological soil and sediment micromorphology* (pp. 155–163). Wiley Blackwell.

Wang, J., Simoneit, B. R. T., Sheng, G., Chen, L., Xu, L., Wang, X., Wang, Y., & Sun, L. (2017). The potential of alkyl amides as novel biomarkers and their application to paleocultural deposits in China. *Scientific Reports*, *7*, 14667. https://doi.org/10.1038/s41598-017-15371-z

WRB. (2015). *World reference base for soil resources 2014, update 2015 International soil classification system for naming soils and creating legends for soil maps*. World Soil Resources Reports No. 106. FAO, Rome. fao.org/3/i3794en/I3794en.pdf

Yost, C. (2008). Phytolith analysis of feature fill samples from the El Dornajo site, Ecuador. Golden, Colorado. *Paleo Research Institute Technical Report*, *8*, 129, 1–18. http://phytolithreport.pdf

SUPPORTING INFORMATION

Additional supporting information can be found online in the Supporting Information section at the end of this article.

How to cite this article: Gebhardt, A., Poszwa, A., Mansuy-Huault, L., Robin, V., Vrydaghs, L., & Lorgeoux, C. (2023). 'Paleoenvironmental study of modern charcoal making activity on forest soils in the Northern Vosges Mountains (Bitche, France): A multidisciplinary study of two remaining charcoal platforms and associated soils sequences' *Geoarchaeology*, 1–25. https://doi.org/10.1002/gea.21986